N72-25377

EXPERIMENTAL APPROACHES TO REMOTE ATMOSPHERIC PROBING IN THE INFRARED FROM SATELLITES

William R. Bandeen
Goddard Space Flight Center
National Aeronautics and Space Administration
Greenbelt, Maryland

ABSTRACT

Remote atmospheric probing in the infrared from satellites had its inception in October 1959 with the launch of Explorer VII carrying a simple wide field radiometer. Since that time much progress has been made in developing radiometric instruments of increasing spatial and spectral resolution. Thirteen different types of radiometric instruments either have been flown in orbit or are scheduled to fly on forthcoming satellites. A fourteenth type, a Very High Resolution Radiometer for Geosynchronous Altitude, is among several of the others whose development has been stressed for the Global Atmospheric Research Program (GARP) of the next decade. Hence, even though it is not yet approved for flight, this instrument is included in this survey of experimental approaches to remote atmospheric probing in the infrared from satellites, developed during the first decade of the space age.

Characteristics of each radiometric instrument and some applications of the different types of data are discussed.

EXPER. APPROACHES INFRARED PROBING FROM SATELLITES

1. INTRODUCTION

The era of remote atmospheric probing in the infrared from satellite began nearly ten years ago with the launch of Explorer VII carrying a rather simple array of hemispheric, omnidirectional sensors to measure the radiation balance of the earth. Since that time radiometric instruments of increasing spatial and spectral resolution, and hence of increasing complexity, have been flown in orbit on the TIROS and NIMBUS research satellites or scheduled for forthcoming flights through the remainder of the decade. With the orbital flight of these instruments has come a concurrent research effort to analyze and interpret the large amounts of radiation data acquired over the entire globe in terms of their physical significance. In addition to the objective of increasing our knowledge of atmospheric processes, a primary objective of these efforts is to develop instrumentation and techniques suitable for the national operational meteorological satellite system. Only recently have flat plate, wide field radiometers been added to the television instrumentation on the ESSA (Environmental Survey SAtellite) operational satellites. The Goddard Space Flight Center/NASA will soon transmit electrically to the National Environmental Satellite Center/ESSA the High Resolution Infrared Radiometer (HRIR) data from NIMBUS III for preliminary operational use, and as an outgrowth of the research and development program three different types of radiometers are now being developed expressly for use on the second generation operational satellites.

The purpose of this paper is to survey the first ten years of remote atmospheric probing in the infrared from satellites. It was deemed advisable to include only those radiometric instruments–thirteen different types in all–which either have flown in orbit or are approved and scheduled for forthcoming flights. One exception was made. A fourteenth instrument, a Very High Resolution Radiometer for Geosynchronous Altitude, was included even though it is not yet part of an approved mission because of its importance to the concept of the Global Atmospheric Research Program (GARP) in the 1970's and because of the advanced technological developments involved in its design.

No attempt has been made to discuss each instrument and its results in detail. Rather the author's objective has been to present a broad overview, giving selected characteristics of each instrument which are of primary interest to the meteorologist or atmospheric physicist, and giving examples of the many possible applications of the data from the different instruments. An attempt has been made to list a comprehensive

---

Editor's Note

"Experimental Approaches to Remote Atmospheric Probing in the Infrared from Satellites" by William R. Bandeen, was written and distributed in advance to members of the National Academy of Sciences Panel on Remote Atmospheric Probing in preparation for a meeting of the Panel in Chicago on 16 May 1968. In writing the document it was presupposed that the Nimbus B spacecraft – carrying radiometric instruments numbered 4, 5, 6a, and 7a in Table I – would be placed successfully in orbit and thereby designated "Nimbus III" within a very few days of the meeting.

Because of a malfunction of the first stage of the rocket vehicle during the launch phase on 18 May 1968, the Nimbus B spacecraft was not placed in orbit. Therefore, all references in Table I and throughout the text to radiometric instruments having been flown on Nimbus III in May 1968 are erroneous.

A "Nimbus B2" mission which will carry the Nimbus B backup instruments numbered 4, 5, 6a, and 7a in Table I was authorized by the National Aeronautics and Space Administration on 27 June 1968. Nimbus B2 is scheduled to be launched in May 1969 and, if successfully injected into orbit, will be designated Nimbus III. The original report as reproduced herein should be read in this context.

bibliography wherein the reader may pursue a deeper interest in the design of a particular instrument or system or in particular applications of the different types of data.

2. BASIS FOR REMOTE ATMOSPHERIC PROBING

The basis for remote atmospheric probing in the infrared lies in the molecular absorption bands of the various gaseous constituents. The principal infrared absorber in the atmosphere is the variable gas H_2O with strong vibration-rotation bands centered near 1.1 microns, 1.38 microns, 1.87 microns, 2.7 microns, and 6.3 microns, and with a rotation band becoming effective, though weak, near 12 microns and intensifying increasingly out to about 65 microns. A second gaseous absorber of importance is CO_2 with strong vibration-rotation bands centered near 2.7 microns, 4.3 microns, and 15 microns. Of particular importance to the concept of remotely sounding vertical profiles of temperature (and, as a subsequent step, the remote sounding of vertical profiles of the variable gases) is the observed constant (or nearly so) mixing ratio of CO_2 from the surface to the vicinity of the mesopause. (This characteristic of the atmosphere is of primary importance to the application of radiometric instruments numbered 6, 7, 9, 10, and 12 in Table 1, all of which are intended for vertical sounding of the atmosphere.) Another important absorber is the variable gas O_3 with a strong vibration-rotation band centered near 9.6 microns. In addition to the bands mentioned above, there are many other bands of H_2O, CO_2, and O_3 and of other gaseous constituents of the atmosphere, but they are not important for purposes of this discussion.

Infrared absorption spectra for the terrestrial atmosphere out to 15 microns are shown in Figure 1. The specific bands mentioned above are clearly identifiable along with other lesser bands. Also, of importance to remote sounding are the atmospheric "windows" where gaseous absorption is minimal. Two windows of consequence to the discussions of instruments that follow are one in the interval 3.5-4.1 microns and another (except for the absorption due to O_3) in the interval 8.0-12.5 microns (cf. Figure 1).

Also of importance to remote atmospheric probing in the infrared are the absorption and scattering characteristics of liquid water droplets and ice crystals making up clouds and of other particulates in the atmosphere (see, for example, the discussion of the Filter Wedge Spectrometer below; No. 10 in Table 1).

3. RADIOMETRIC INSTRUMENTS FOR REMOTE ATMOSPHERIC PROBING IN THE INFRARED FROM SATELLITES

The fourteen types of radiometric instruments mentioned above and some examples of data from final satellite-borne or preliminary balloon-borne or aircraft-borne versions of the instruments are discussed in this Section. As previously pointed out, the discussion of a particular instrument and its data in a survey of this type must necessarily be limited, and an attempt has been made to include a sizeable bibliography to which the reader can refer for additional information. It was not possible to conduct an exhaustive literature search in compiling the bibliography. Rather it was assembled largely from sources immediately available to the author, and hence it seems inevitable that many excellent references have been inadvertently omitted. For these omissions the author should like to express his sincere regrets.

Table I
Radiometric Instruments for Remote Atmospheric Probing in the Infrared from Satellites

	No.	Radiometric Instrument	Satellite(s) (See Note A.)	Channel(s)	Detector(s)	Instantaneous Field of View (degrees of arc)	Linear Resolution at Subsatellite Point from (Nominal Orbital Height) for Indicated Satellite(s) (both in Km)	Application
Flown in Orbit (as of May 1968)	1.	WIDE FIELD Sensors (See Note B.)	Explorer VII, TIROS III, IV, VII ESSA 3, 5, . . . etc.	1) Black (Long - and Short - Wave Radiation 2) White (Long - Wave Radiation)	Hemispheres or Flat Plates — Thermistor Bolometers	Entire Earth's Disc	~50% from 1400(700) Expl., TIROS 2400(1400) ESSA	Radiation Balance (Long - Wave Emission, Albedo)
	2.	Two Cone Low Resolution Radiometer	TIROS II, III, IV	1) Black (Long - and Short - Wave Radiation) 2) White (Long - Wave Radiation)	Thermistor Bolometers	50°	670 (700)	Radiation Balance
	3.	Medium Resolution Radiometer [Scanning]	TIROS II, III, IV, VII	1) 6.0 - 6.5μ (TIROS II, III, IV) 14.8 - 15.5μ (TIROS VII) 2) 8.0 - 12.0μ 3) 0.2 - 6.0μ 4) 8.0 - 30.0μ (Not on TIROS IV) 5) 0.55 - 0.75μ	Thermistor Bolometers	5°	60 (700)	Cloud Cover Mapping Storm Tracking Surface Temp. Cloud Top Heights Radiation Balance Tropospheric Water Vapor Stratospheric Temp. and Circulation
	4.	High Resolution Infrared Radiometer (HRIR) [Scanning]	Nimbus I, II, III	1) 3.5 - 4.1μ (Nimbus I, II) 3.5 - 4.1μ 0.7 - 1.3μ (Nimbus III)	Pb Se Single - Stage, Radiatively - Cooled to 200°K	0.46°	9 (1100)	Cloud Cover Mapping Storm Tracking Surface Temp. Cloud Top Height (Absolute Emission Measurements, Nighttime Only)
	5.	Medium Resolution (Infrared) Radiometer (MRIR) [Scanning]	Nimbus II, III	1) 6.4 - 6.9μ 2) 10.0 - 11.0μ 3) 14.0 - 16.0μ (Nimbus II) 14.5 - 15.5μ (Nimbus III) 4) 5.0 - 30.0μ (Nimbus II) 20.0 - 23.0μ (Nimbus III) 5) 0.2 - 4.0μ	Thermistor Bolometers	2.9°	55 (1100)	Cloud Cover Mapping Storm Tracking Surface Temp. Cloud Top Heights Radiation Balance Tropospheric Water Vapor Stratospheric Temp. and Circulation
	6a.	Infrared Interferometer Spectrometer (IRIS)	Nimbus III	1) 5 - 20μ; Spectrally Scanning; Resolution $\Delta\nu = 5\,cm^{-1}$ ($\Delta\lambda = 0.1\mu$ @ 15μ)	Thermistor Bolometer	8°	150 (1100)	Vertical Profiles (Temp., H_2O, O_3, etc.)
	7a.	Satellite Infrared Spectrometer (SIRS)	Nimbus III	Total of 8 Chans: 7 in 15μ CO_2 Band; 1 in 11μ Window; Resolution $\Delta\nu = 5\,cm^{-1}$	Thermistor Bolometers	12°	230 (1100)	Vertical Temp. Profile
	8.	ITOS High Resolution Radiometer [Scanning]	TIROS M ITOS A, B, . . . etc.	1) 10.5 - 12.5μ 2) 0.52 - 0.73μ	Thermistor Bolometer Silicon Cell	0.30° 0.16°	7 4 (1400)	Cloud Cover Mapping Storm Tracking Surface Temp. Cloud Top Heights Albedo
	6b.	IRIS	Nimbus D	1) 6.3 - 50μ; Spectrally Scanning; Resolution $\Delta\nu = 3.0\,cm^{-1}$ ($\Delta\lambda = 0.07\mu$ @ 15μ)	Thermistor Bolometer	5°	90 (1100)	Vertical Profiles (Temp., H_2O, O_3, etc.)

Under Development for Forthcoming Flights	7b.	SIRS	Nimbus D	Total of 14 Chans: 7 in 15μ CO_2 Band; 6 in Rot. H_2O Band; 1 in 11μ Window; Resolution $\Delta\nu$ = 5 cm	Thermistor Bolometers	12°	230 (1100)	Vertical Profiles (Temp., H_2O)	
	9.	Selective Chopper Radiometer (SCR)	Nimbus D	Total of 6 Chans: 6 in 15μ CO_2 Band; 1 Switchable to 11μ Window	Thermistor Bolometers	10°	190 (1100)	Vertical Temp. Profile	
	10.	Filter Wedge Spectrometer (FWS)	Nimbus D	1) 1.2 - 2.4μ; 3.2 - 6.4μ Spectrally Scanning; Resolution $\lambda/\Delta\lambda$ = 100 ($\Delta\lambda$ = 0.05μ @ 5μ)	Pb Se Single - Stage, Radiatively - Cooled to 160°K	2°	38 (1100)	Determine Liquid Water or Ice Content of Clouds (1.2 - 2.4μ) Vertical Temp. Profile (4.3μ CO_2 Band) Vertical H_2O Profile (6.3μ H_2O Band)	
	11.	Temperature Humidity Infrared Radiometer (THIR) [Scanning]	Nimbus D	1) 10.5 - 12.5μ 2) 6.5 - 7.0μ	Thermistor Bolometers	0.40° 1.20°	8 23 (1100)	Cloud Cover Mapping Storm Tracking Surface Temp. Cloud Top Heights Air Mass Discrimination — Vertical Motion Jet Stream Location	
	12.	ITOS Vertical Temp. Profile Radiometer (VTPR)	ITOS (1970's)	Total of 8 Chans: 6 in 15μ CO_2 Band; 1 in Rot. H_2O Band; 1 in 11μ Window	Thermistor Bolometer (Filter Wheel in Front of One Detector)	2°	50 (1400)	Vertical Temp. Profile	
	13.	ITOS Very High Resolution Radiometer (VHRR) [Scanning]	ITOS (1970's)	1) 10.5 - 12.5μ 2) 0.6 - 0.7μ	Hg Cd Te; 2 - Stage Radiatively - Cooled to 80°K Photodiode	0.034°	0.8 (1400)	Cloud Cover Mapping Storm Tracking Surface Temp. Cloud Top Heights Albedo	
Proposed	14.	Very High Resolution Radiometer for Geosynchronous Altitude [Scanning]	Geosynchronous Satellite (Planning Only — Not An Approved Mission)	1) 10.5 - 12.5μ	Hg Cd Te; Cryogenically Cooled to 80°K	0.023°	15 (35,800)	Cloud Cover Mapping Storm Development/Tracking Surface Temp. Cloud Top Heights Upper Level Winds	

Note A. Launch Dates for U. S. Meteorological Satellites Carrying Infrared Radiometric Instruments (Through 1970)

Explorer VII	13 October 1959	
TIROS II	23 November 1960	
TIROS III	12 July 1961	
TIROS IV	8 February 1962	
TIROS VII	19 June 1963	
Nimbus I	28 August 1964	
Nimbus II	15 May 1966	
ESSA 3	2 October 1966	
ESSA 5	20 April 1967	(Future odd-numbered ESSA satellites will carry wide field sensors. Additional ESSA satellites will be launched as required for the National Operational Meterological Satellite System.)
Nimbus III	May 1968	
TIROS M	1st Quarter 1969	(First of the Improved TIROS Operational Satellites — ITOS)
ITOS A	3rd Quarter 1969	(Followed by ITOS B, C, . . . as required for the National Operational Meteorological Satellite System in the 1970's)
Nimbus D	1st Quarter 1970	

Note B. Wide field sensors will also be flown on the second-generation operational meterological satellites: TIROS M, ITOS A, B, C....

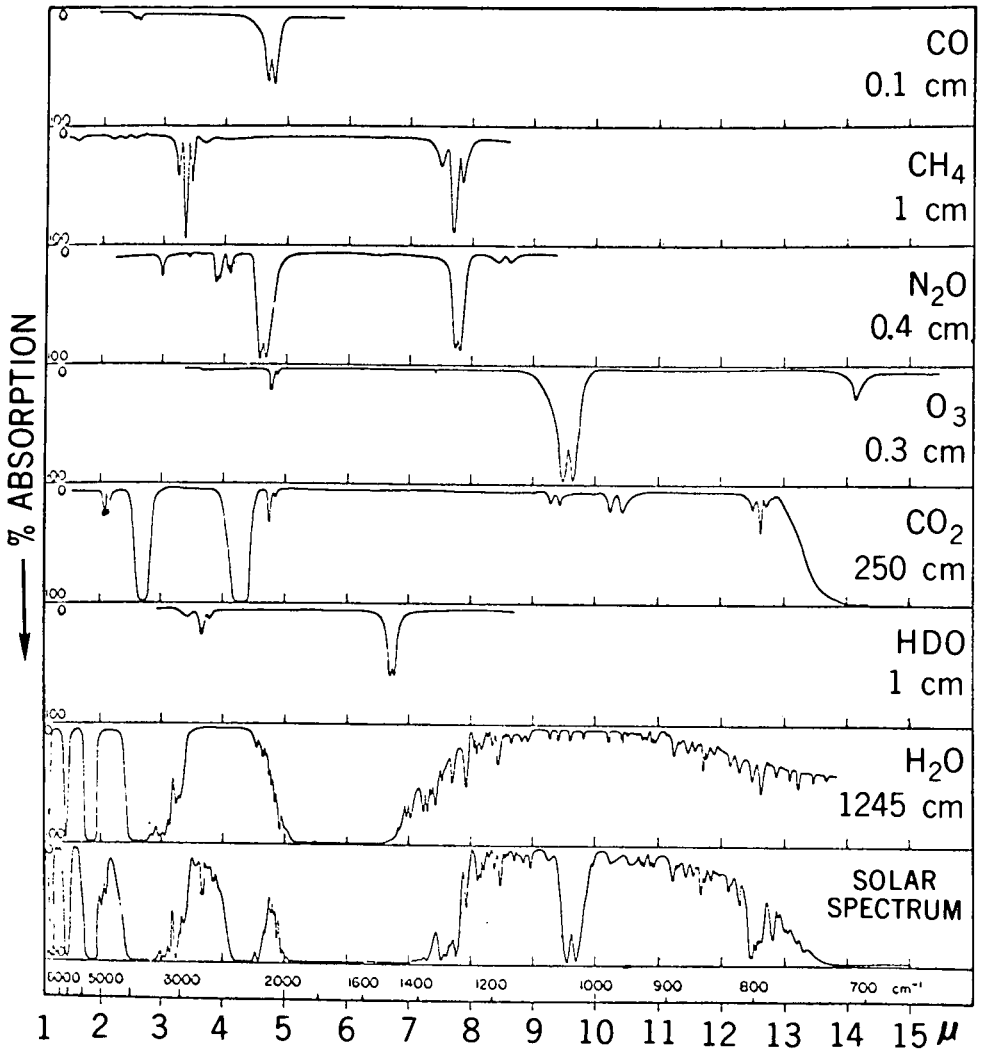

Figure 1. The near-infrared solar spectrum (bottom curve). Other curves are laboratory spectra of the molecules indicated. The approximate abundance of each gas in terms of cm NTP is indicated under the corresponding chemical formula; these are representative values for the highly variable gases H_2O and O_3 (After Howard, Burch, and Williams, 1955).

The fourteen instruments and selected characteristics pertaining to them are listed in Table 1. This table virtually forms an outline of the paper, and it is intended that the reader refer to it often.

3.1 Wide Field Sensors

The first satellite-borne instrument to probe the atmosphere in the infrared was the thermal radiation balance experiment carried by the Explorer VII Satellite, launched on 13 October 1959 (Suomi, 1961; cf. Table 1, No. 1). This experiment, originally part of the International Geophysical Year 1957-58 Earth Satellite Program, was designed to measure the balance between long-wave radiation lost to space and short-wave solar radiation absorbed by the earth and atmosphere (Suomi, 1958). The resulting excesses and deficits in the radiation balance, and their spatial and temporal variations, make available the potential energy to drive the general circulation of the global atmospheric

"heat engine." Hence, their study is of primary importance in acquiring a deeper understanding of the thermal and dynamical characteristics of the atmosphere.

Explorer VII carried five hemispheric sensors in the form of hollow silver hemispheres. The hemispheres were thermally isolated from but in close proximity to special aluminized mirrors. The image of the hemisphere which appeared in the mirror made the sensor look like a full sphere. The spin of Explorer VII made the mirror-backed hemispheres act essentially as isolated spheres in space. Two of the hemispheres were provided with a black coating which made them respond about equally to solar and terrestrial radiation. One hemisphere was coated white, making it more sensitive to terrestrial radiation than to solar radiation. A fourth was gold-coated, making it more sensitive to solar radiation than to terrestrial radiation. The fifth hemisphere was tabor-surfaced and equipped with a shade to protect it from direct sunlight. In addition, a black sphere was mounted on the axis of the satellite at the top. It was used to determine any deterioration in the mirror surfaces by comparison with the blackened hemispheres. All temperature sensing elements were thermistors. The information telemetered to the earth was the sensor temperatures. The long-wave and short-wave radiation values were obtained by using these temperatures in heat balance equations. Even though the Explorer VII sensors viewed the entire earth's disc, the effective spatial resolution was considerably reduced by geometrical considerations, i.e., about 50% of the energy received at the nominal orbital height of 700 km originated within a radius of about 700 km from the subsatellite point.

An analysis of the nocturnal long-wave radiation lost to space as measured by the hemispheric sensors on Explorer VII is shown in Figure 2 (Weinstein and Suomi, 1961).

A variation of the Explorer VII experiment has been flown on several of the TIROS satellites which are also spin stabilized. In this variation a pair of hemispheric shells made of aluminum sheeting and backed by mirrors was used, one hemisphere with a black surface and the other with a white surface (House, 1965; Suomi, et al., 1966). Another variation of the experiment is currently being flown on the odd-numbered ESSA satellites of the operational meteorological satellite system. (The ESSA satellites use the same basic spinning spacecraft as did the TIROS II, III, IV, and VII satellites. But whereas the spin axes of these TIROS satellites lay approximately within the orbital plane, the spin axes of the ESSA satellites are perpendicular to the orbital plane, causing them to be likened to a "cartwheel, rolling around the orbit.") In this variation flat plate sensors are used instead of hemispheres. Further, two versions of the flat plate sensors have been developed: (1) the basic radiometer consisting of one black and one white flat disc, and (2) the basic radiometer with cone optics added to restrict the field of view (Nelson and Parent, 1965; Operational Satellites Office, 1968). Because of the cosine dependence of a flat surface and because of the cone optics, the effective spatial resolution on the earth of the flat plate radiometer is less than that of an omnidirectional hemisphere for which the "Linear Resolution" values in Table 1, No. 1 were calculated. However, the principles applying to all variations are the same and the purpose of both the hemispheric and the flat plate sensors is to obtain low resolution measurements of the radiation balance of the earth-atmosphere system (Vonder Haar, 1968).

3.2 Two Cone Low Resolution Radiometer

A low resolution unchopped radiometer was flown on the TIROS II, III, and IV satellites (cf. Table 1, No. 2). The purpose of this radiometer was to measure the

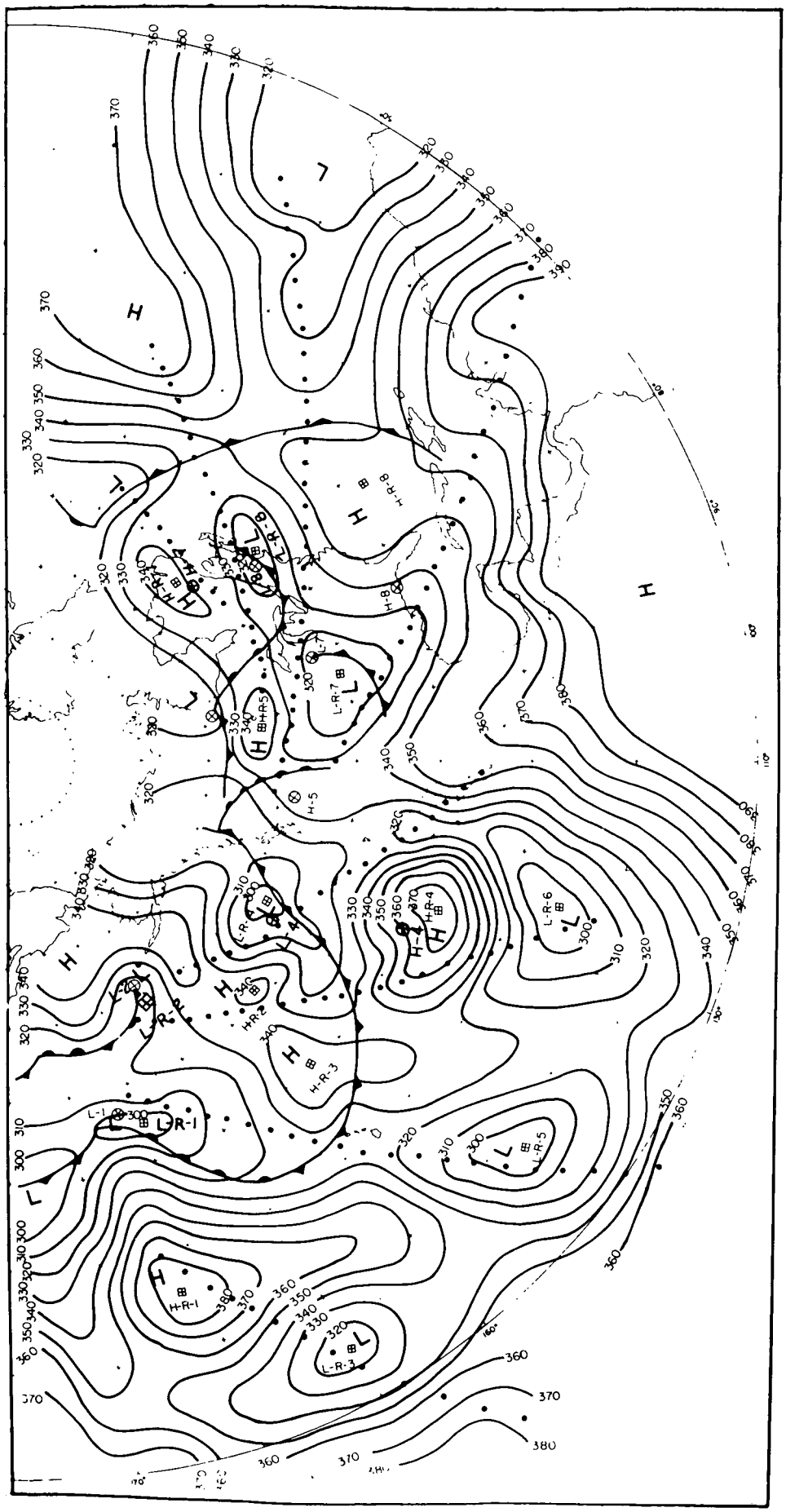

Figure 2. Long-wave radiation loss map, December 1, 1959. Lines are isolangleys, connecting equal long-wave radiation loss values in Langleys per minute x 10^{-3}. Surface pressure centers and fronts are composite to the satellite passage time. Surface pressure centers, marked by circles, are designated L for Low and H for High, plus an arabic number (thus L-1). Radiation centers, marked by squares, are distinguished from surface centers by the inclusion of R (thus L-R-1 is radiation Low number 1 which is associated with surface Low L-1). Satellite observations points and orbit path are shown by dots (After Weinstein and Suomi, 1961).

equivalent blackbody temperature and albedo of the earth within its 50° field of view which was coaxial with the spin axis and with the optical axes of the two television cameras on the satellite (Bandeen, Hanel, et al., 1961).

The two low resolution channels consisted of a black and white thermistor detector each mounted in the apex of a highly reflective mylar cone. The black detector was equally sensitive to long-wave terrestrial radiation and reflected sunlight. The white detector was coated to be reflective in the visible and near infrared. The differences in the spectral emissivities of the two detectors yielded two independent energy balance equations from which the two unknowns, the equivalent blackbody temperature and the albedo within the field of view, could be solved (Hanel, 1961). The data analysis procedures and examples of analyzed data have been discussed by Bartko, Kunde, et al. (1964).

3.3 Medium Resolution Radiometer (TIROS)

In order to map radiometric data at considerably higher spatial resolutions than are possible with the two previously discussed instruments, the instantaneous field of view must be made smaller and it must be caused to scan over the earth beneath the satellite. The first radiometer of this type was the five-channel, medium resolution scanning radiometer flown on the TIROS II satellite, launched on 23 November 1960 (cf. Table 1, No. 3). The optical axes of the five channels were parallel and inclined by 45 degrees to the spin axis of TIROS. Viewing in both directions, they swept out two 45-degree half-angle cones around the spin axis on the "top" and "bottom" of the spacecraft as it spun at about 10 RPM. The intersection of these cones with the earth defined scan lines of varying shapes (depending upon the instantaneous nadir angle of the spin axis), and the progression of the satellite in orbit caused the advance of the individual scan lines. On the ground, then, it was possible to reconstruct the data in the form of maps of outgoing radiance in the direction of the satellite. The design of this radiometer has been described by Bandeen, Hanel, et al. (1961). The broad-band spectral intervals of the five channels and the nature of the radiation sensed are listed below:

1. 6.0-6.5 microns; water vapor absorption
2. 8.0-12.0 microns; atmospheric window
3. 0.2-6.0 microns; reflected solar radiation
4. 8.0-30.0 microns; thermal radiation
5. 0.55-0.75 microns; visible radiation (similar to the response of the television cameras)

The physical significance of these spectral regions has been discussed by Hanel and Wark (1961).

The same type of radiometer was subsequently flown on the TIROS III, TIROS IV, and TIROS VII satellites with several modifications. The most significant of these was the substitution of a channel responding to radiation in the interval 14.8-15.5 microns in lieu of the 6.0-6.5 micron channel on TIROS VII. The substitute channel sensed radiation within the 15 micron absorption band of carbon dioxide (cf. Fig. 1). The physical significance of this region has been reported by Hanel, et al. (1963), Bandeen, et al. (1963a), Nordberg, et al. (1965), and Warnecke (1966a). Detailed descriptions of the radiometers and of the available data are given in appropriate Manuals and Catalogs for each satellite (see, for example, Staff Members, 1964).

The synoptic analysis of infrared data, including the mapping of cloud systems, the tracking of storms, and the inference of cloud top heights, both night and day, has received the attention of many workers. A sampling of studies in these areas includes papers by Fritz and Winston (1962), Nordberg, et al. (1962), Bandeen, et al. (1963b), Rao and Winston (1963), Allison, et al. (1964), Bandeen, et al. (1964), Hawkins (1964), Rasool (1964), Warnecke (1966b), Widger, et al. (1966), Allison and Thompson (1966b), Allison and Warnecke (1966c), and Allison and Warnecke (1967). Winston (1965) questioned some of the results of Rasool's (1964) analysis.

Allison and Warnecke (1967) interpreted synoptically the satellite-detected global radiation patterns in terms of a conventional weather analysis. Figure 3, taken from their paper, shows the equivalent blackbody temperature (T_{BB}, °K) pattern of outgoing 8.0-12.0 micron radiation from the earth's surface and the clouds above it measured by TIROS VII during the northern hemisphere winter and southern hemisphere summer. The cold areas which lie poleward of the 35 N and 40 S parallels are related to extratropical cyclonic activity; those near the equator indicate high cloud systems associated with the intertropical convergence zone. The presence of tropical cyclone "Danielle" under the high cloud shield at 40 S, 65 E indicates the beginning of hurricane activity in the southern hemisphere. The original figure, published by the authors in seven colors, was more impressive and informative than the black-and-white reproductions shown here.

The inference of ground surface temperatures from TIROS 8.0-12.0 micron measurements has been discussed by Wark, Yamamoto, and Lienesch (1962), Fritz (1963), and Buettner and Kern (1963). A promising method of specifying 500-mb heights from TIROS 8.0-12.0 micron data has been reported by Jensen et al. (1966), and correlations between TIROS 8.0-12.0 micron data and some diabatic properties of the atmosphere have been discussed by Davis (1965).

A method for inferring the mean relative humidity of the upper troposphere from coordinated measurements of the 6.0-6.5 micron and 8.0-12.0 micron channels was developed by Möller and Raschke (1964). An extension of this method to infer the water vapor mass above the 500-mb level, using conventional 500-mb temperature data in addition to the satellite data, was discussed by Bandeen, et al. (1965) and Bandeen (1966). Analyses of tropospheric moisture content utilizing this method have been published by Raschke (1967), Raschke and Bandeen (1967a), and Raschke and Bandeen (1967b). Figure 4 shows a map of the total water vapor mass above 500 mb in February 1962 determined by this method (Raschke and Bandeen, 1967b). The patterns indicate that the highest amounts of precipitable water vapor occur in the tropics and, particularly, in three regions, vis., Southeast Asia, South America, and Central Africa. Fritz and Rao (1967), using data from the comparable "water vapor" and "window" channels of the NIMBIS II MRIR (cf. Table 1, No. 5) and conventional radiosonde data, discussed on both observational and theoretical grounds the problems involved in attempting to estimate atmospheric water vapor content above high clouds, especially cirrus, from such satellite measurements. In their discussion Fritz and Rao questioned some of the findings of Raschke and Bandeen (1967b).

A method for converting the 8.0-30.0 micron or 8.0-12.0 micron radiance measurements to total outgoing long-wave radiative flux was derived by Wark, et al. (1962). The original method, which employed a theoretically-determined limb darkening function, has

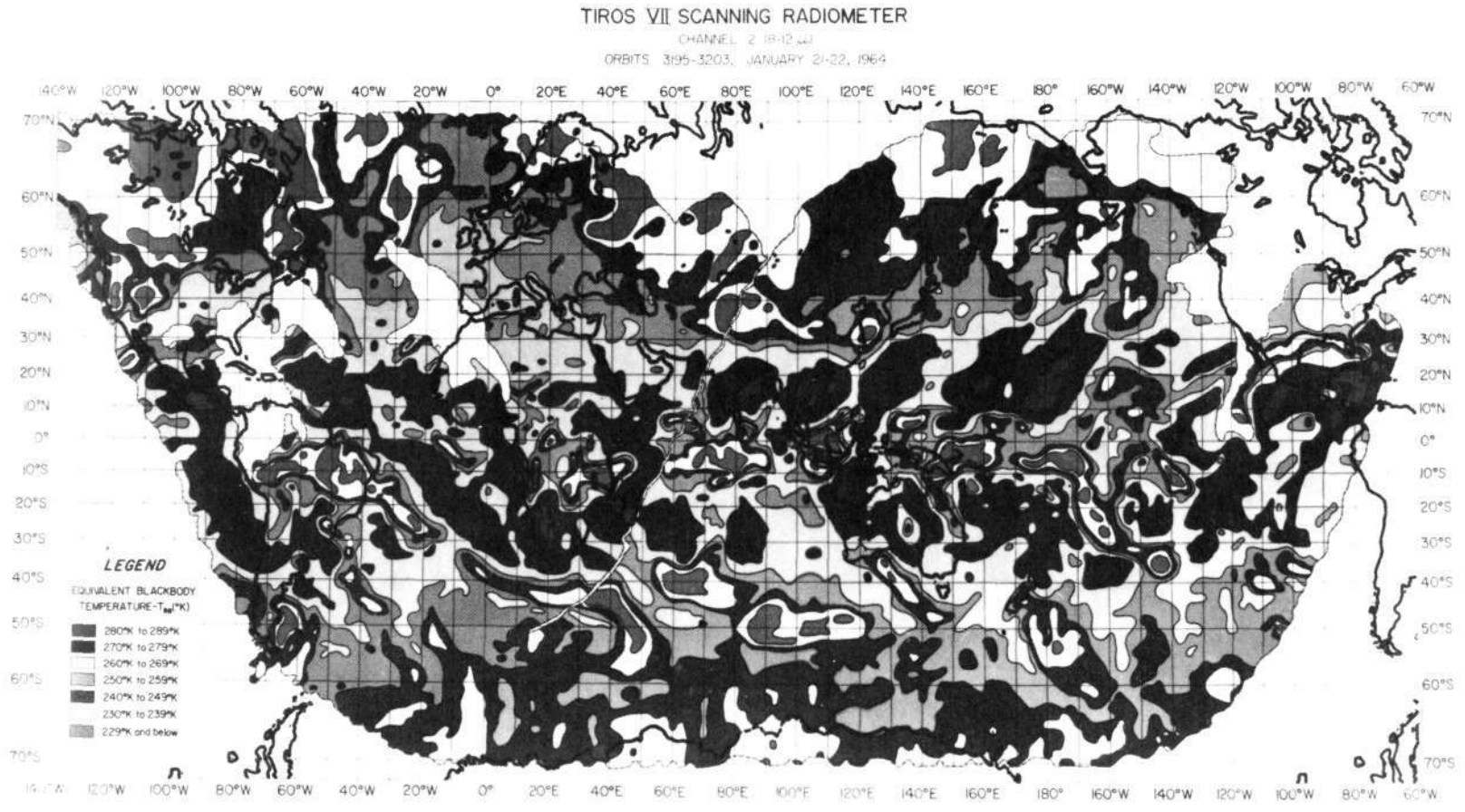

Figure 3. Composite map of radiation measured by the 8.0–12.0 micron channel of TIROS VII during nine consecutive orbits on January 21–22, 1964 (After Allison and Warnecke, 1967). The published figure is in seven shades of color.

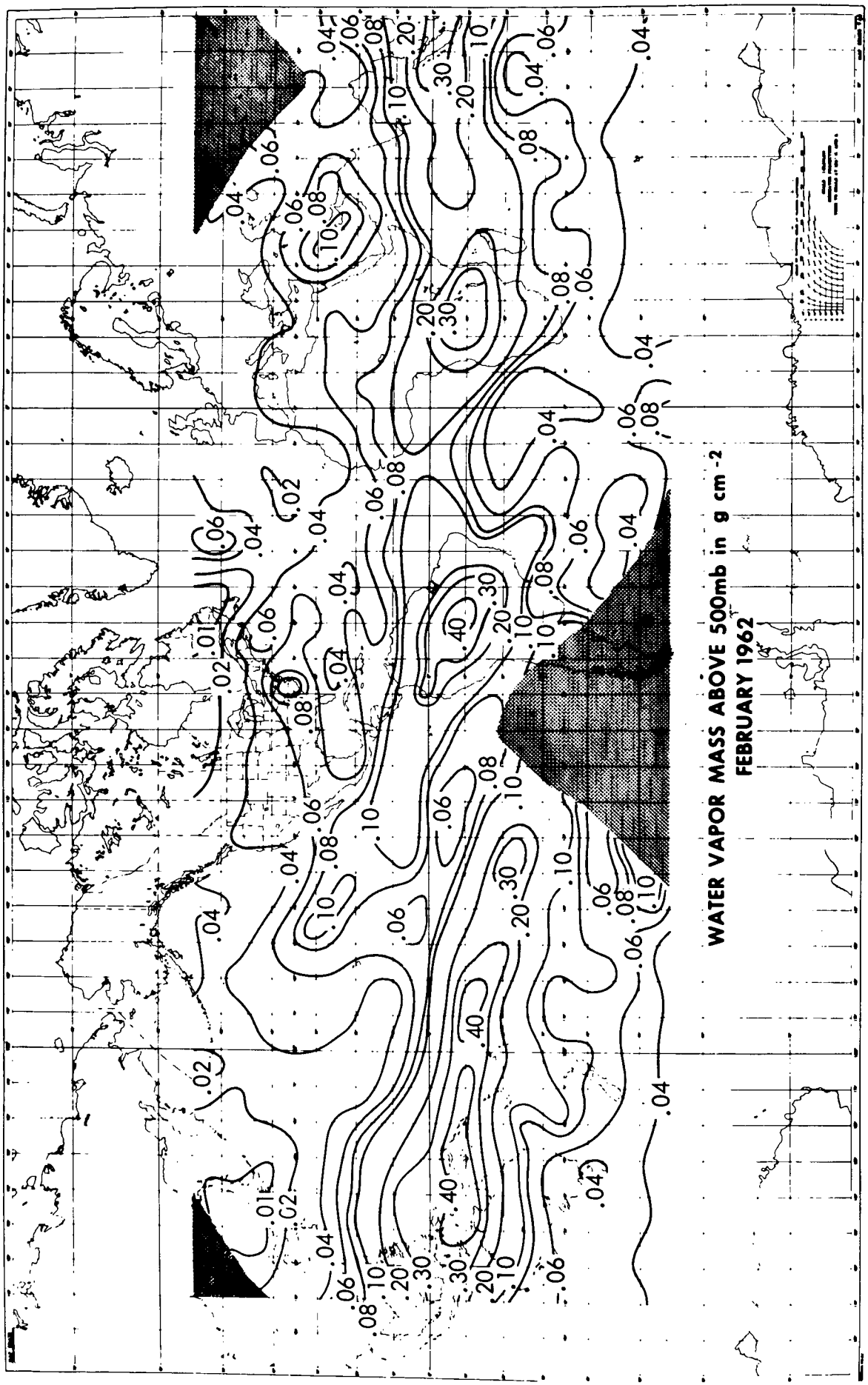

Figure 4. Quasi-global distribution of the water vapor mass above 500 mb during February 1962 inferred from coordinated TIROS IV 6.0–6.5 micron and 8.0–12.0 micron radiometric measurements (After Raschke and Bandeen, 1967b).

been improved by the application of a statistically-derived limb darkening function using infrared radiance data from the TIROS II, III, IV, and VII medium resolution scanning radiometers (Lienesch and Wark, 1967).

A number of analyses comparing the total outgoing long-wave radiative flux (deduced by the aforementioned method) with midtropospheric flow patterns, zonal kinetic energy, and available potential energy have been presented by Winston and Rao (1962), Winston and Rao (1963), Winston (1967a) and Winston (1967b). Also, by combining the total outgoing long-wave flux, inferred from the 8.0-30.0 micron or 8.0-12.0 micron measurements, with the albedo, inferred from the 0.2-6.0 micron or 0.55-0.75 micron measurements, analyses of the large-scale radiation balance have been carried out by Bandeen, et al. (1965), Rasool and Prabhakara (1966), and Vonder Haar (1968).

The 14.8-15.5 micron channel carried by the TIROS VII scanning radiometer measures emission from carbon dioxide in the atmosphere (cf. Figure 1). Because of the strength of the 15 micron band and because carbon dioxide is uniformly mixed (at least below the mesopause) in the atmosphere, the weighting function, $d\tau/d \log p$ (where τ is the mean normal transmittance to space over the effective spectral response and p is ambient pressure) of the 14.8-15.5 micron channel peaks at about 20 km (which is slightly higher than the peak of the weighting function for the spectrally broader 14.0-16.0 micron channel of the NIMBUS II MRIR shown in Figure 11). Thus, the 14.8-15.5 micron measurements can be interpreted in terms of mean temperatures of the lower stratosphere. Nordberg, et al. (1965), Warnecke (1966a), and Shen, et al. (1968) have discussed these data and shown that such events as sudden stratospheric warmings can be detected. Belmont, et al. (1968) have shown that a high correlation exists between the TIROS VII 15 micron data and 30 mb atmospheric temperatures. Kennedy and Nordberg (1967) made an harmonic analysis of the circumpolar temperature patterns and derived circulation features from the analysis.

3.4 High Resolution Infrared Radiometer (HRIR)

Nearly an order of magnitude increase in the linear resolution over previous satellite infrared radiometers was achieved with the launch of the first HRIR aboard NIMBUS I on 28 August 1964 (cf. Table 1, No. 4). In contrast to the TIROS medium resolution radiometer, the HRIR required a 45-degree rotating primary mirror to effect the transverse scan from the earth-oriented, three-axis stabilized NIMBUS spacecraft. The design of this instrument has been described by Foshee, et al. (1965). A description of the instrument is also given in the applicable Users' Guides (see, for example, NIMBUS II Users' Guide, 1966). The physical significance of the HRIR equivalent blackbody temperature measurements has been discussed by Kunde (1965), and investigations of the mesoscale resolutions possible and of characteristics of the HRIR data pertinent to such analyses have been carried out by Fujita and Bandeen (1965). Geophysical observations by the HRIR, such as cloud heights and sea surface and soil temperatures, have been discussed by Nordberg (1965), and HRIR measurements over the Antarctic ice pack and other polar features have been reported by Popham and Samuelson (1965).

The meteorological interpretation of HRIR data has been discussed by such authors as Nordberg and Press (1964), Widger, et al. (1965), Widger (1966), Nordberg, et al. (1966), and Allison, et al. (1966a). A photo facsimile depiction of hurricane Gladys and a single analog trace drawn to the same west-to-east scale are shown in Figure 5; hence,

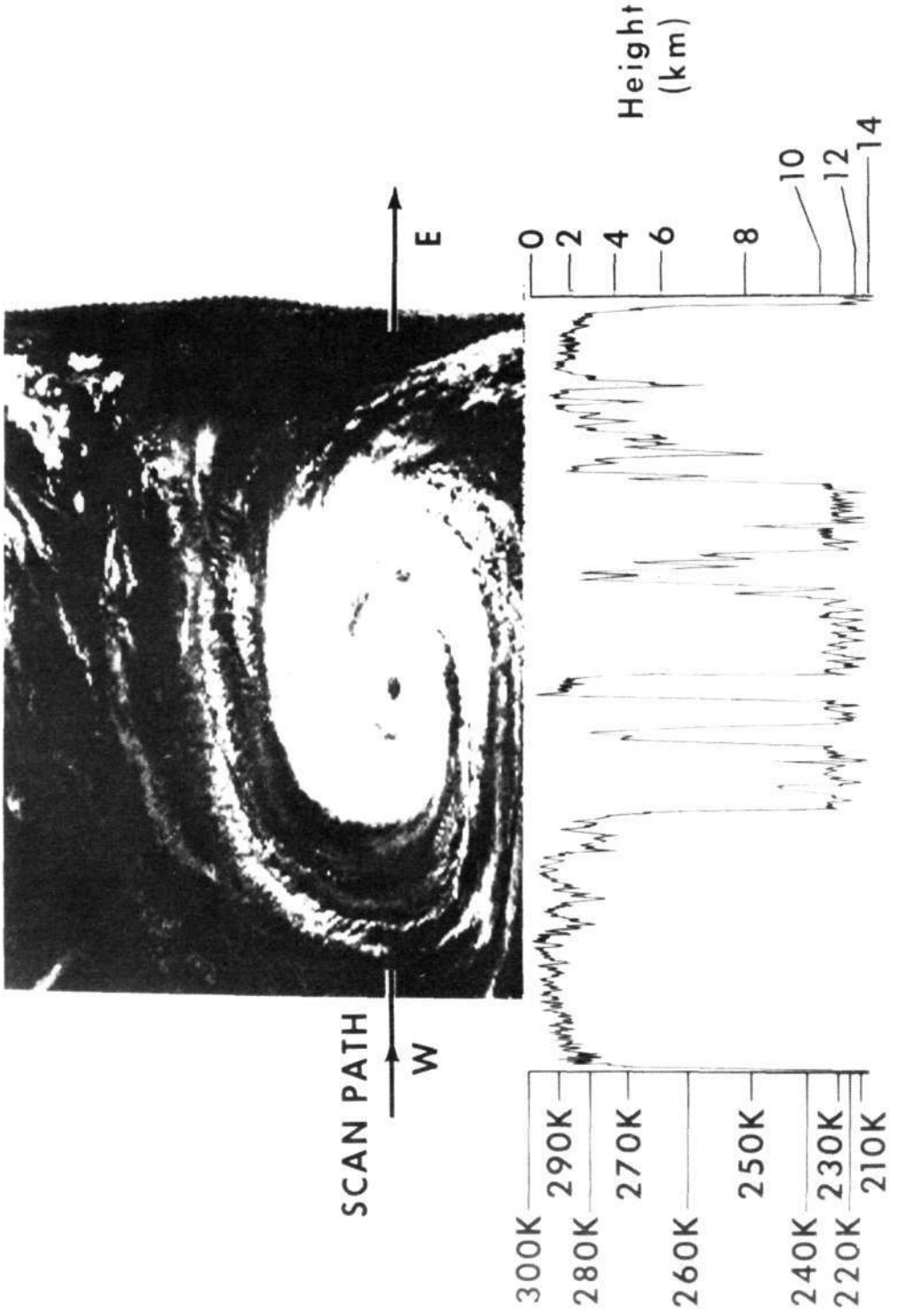

Figure 5. An HRIR depiction of hurricane Gladys at 0422 UT, 18 September 1964. The HRIR photofacsimile picture of the hurricane is compared to a single HRIR analog trace through the eye of the hurricane. The analog trace is related to equivalent blackbody temperature (T_{BB}) values given on the left. Geometric height above sea level is related to T_{BB} values by means of the 0000 UT 18 September 1964 radiosonde sounding from Kindley Air Force Base, Bermuda (After Allison et al., 1966a).

a given feature in the picture corresponds to the same feature in the analog trace underneath. The observed radiation intensities, expressed in °K, are measured along the left hand ordinate. The blackbody temperatures were converted to height on the basis of an actual temperature sounding. The corresponding heights are shown along the right hand ordinate (Allison, et al., 1966a).

The capability of the HRIR to detect and track storms at night is illustrated in Figure 6. Tropical storm Ruby was initially detected by the NIMBUS HRIR at 1500 UT, 31 August 1964, almost 21 hours before aerial reconnaissance located the storm. On four subsequent occasions in the week that followed, the HRIR tracked the course of Ruby across the Pacific until it passed full-blown over Hong Kong and dissipated over mainland China (Allison, et al., 1966a).

Another application of high resolution radiation data is the observation of sea surface temperatures and ocean currents. The importance of the temperature of the sea surface boundary has been emphasized by the Global Atmospheric Research Program (GARP) Report of the Study Conference held in Stockholm (1967). Under clear sky conditions, sea surface temperatures can be determined with an accuracy of ±1 to 2°K (Warnecke, et al., 1968a). The remote detection of the Gulf Stream boundary by the NIMBUS II HRIR is shown in Figure 7, in which temperature gradients of 5° to 10°K over 20 km along the north wall were measured (Warnecke, 1968b).

In addition to the primary stored-data mode of operation, the HRIR experiments on NIMBUS II and III were adapted to the Automatic Picture Transmission (APT) system whereby local reception of the data in real time was possible the world over whenever the spacecraft came within line-of-sight range of a relatively simple and inexpensive groundstation (Nordberg, et al., 1966; Goldshlak, 1968).

Because of the intensity of the solar spectrum in the wavelength interval 3.5-4.1 microns, reflected solar radiation may be appreciable in daytime HRIR measurements, adding to the emitted radiation and making interpretations of the measurements in terms of surface temperatures ambiguous. Thus only nighttime measurements can be interpreted in terms of true surface temperatures. In order to eliminate possible ambiguities in daytime measurements, the NIMBUS III HRIR has a second passband, 0.7-1.3 microns, wherein reflected solar radiation predominates over emission at normal atmospheric and surface temperatures. However, at nighttime, the NIMBUS III HRIR makes measurements of emission only in the interval 3.5-4.1 microns, just as its two predecessors did. (For another view of NIMBUS HRIR data, see Figure 18.)

3.5 Medium Resolution (Infrared) Radiometer (MRIR)

The NIMBUS MRIR was similar in many respects to the earlier TIROS medium resolution scanning radiometer, but it represented an entirely new instrumental design, incorporating a 45-degree rotating primary mirror (similar to that of the HRIR) to effect the transverse scan necessary from the earth-oriented, three-axis-stabilized NIMBUS spacecraft. The first MRIR was launched aboard NIMBUS II on 15 May 1966 (cf. Table 1, No. 5). A description of the instrument is given in the applicable Users' Guides (see, for example, NIMBUS II Users' Guide, 1966).

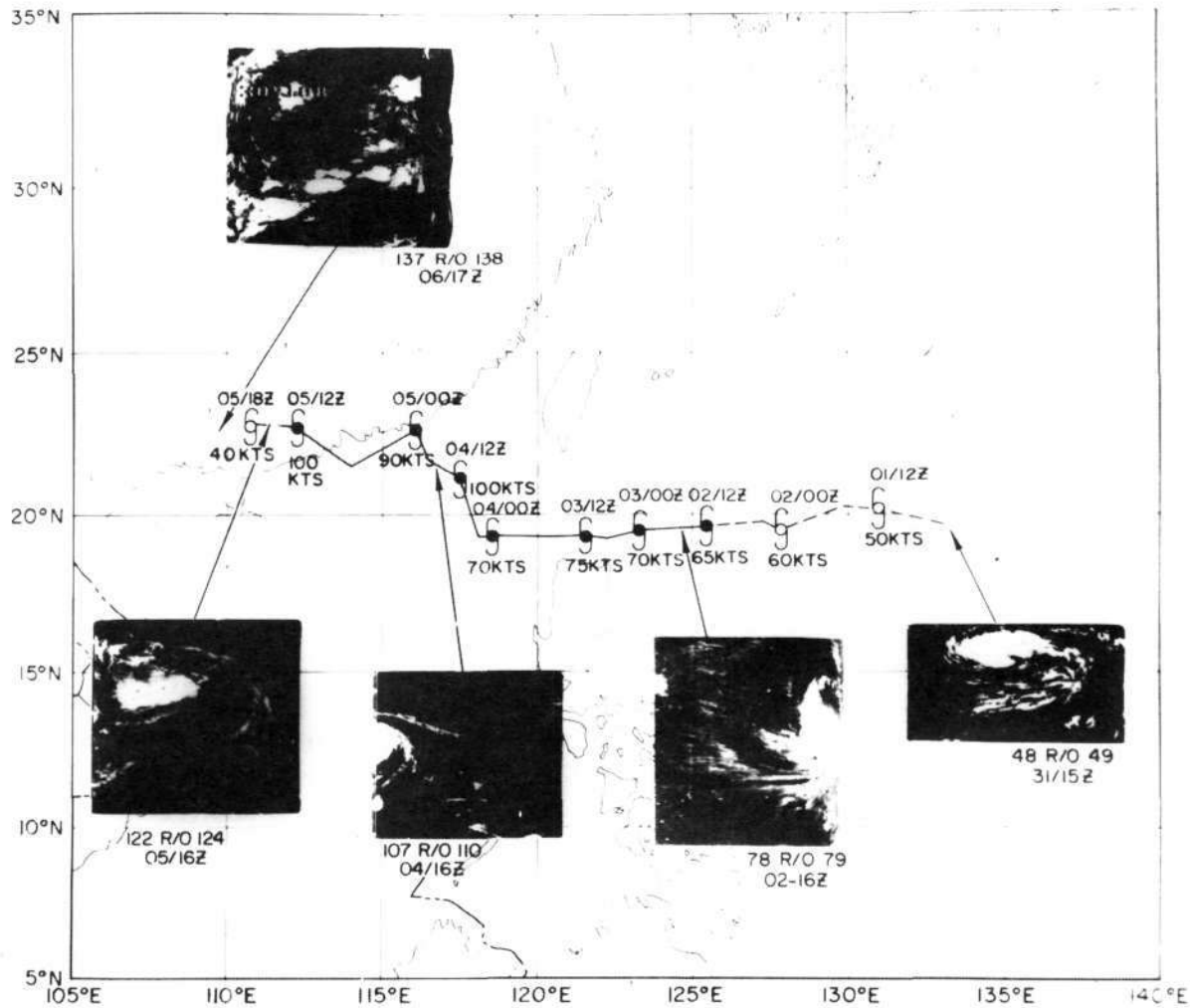

Figure 6. Track of typhoon Ruby from 31 August to 6 September 1964 with inserts of five Nimbus I HRIR photofacsimile depictions of Ruby in the western Pacific Ocean (After Allison et al., 1966a).

The application of the data is very similar to that of the earlier TIROS instrument. An advantage of the NIMBUS MRIR is that it views the entire globe, while the TIROS radiometer did not view poleward of about latitude 63° because of the lower inclination of the TIROS orbit. Global radiation balance studies have been carried out by Möller (1967), Raschke, Möller, and Bandeen (1968), Raschke and Pasternak (1968), and Raschke (1968).

An example of the total outgoing long-wave radiation inferred from the NIMBUS II 5.0-30.0 micron data by the method of Wark et al. (1962) is shown in Figure 8 (Raschke and Pasternak, 1968). The other component of the radiation balance, the absorbed solar radiation, follows from measurements of the albedo and a knowledge of the solar constant.

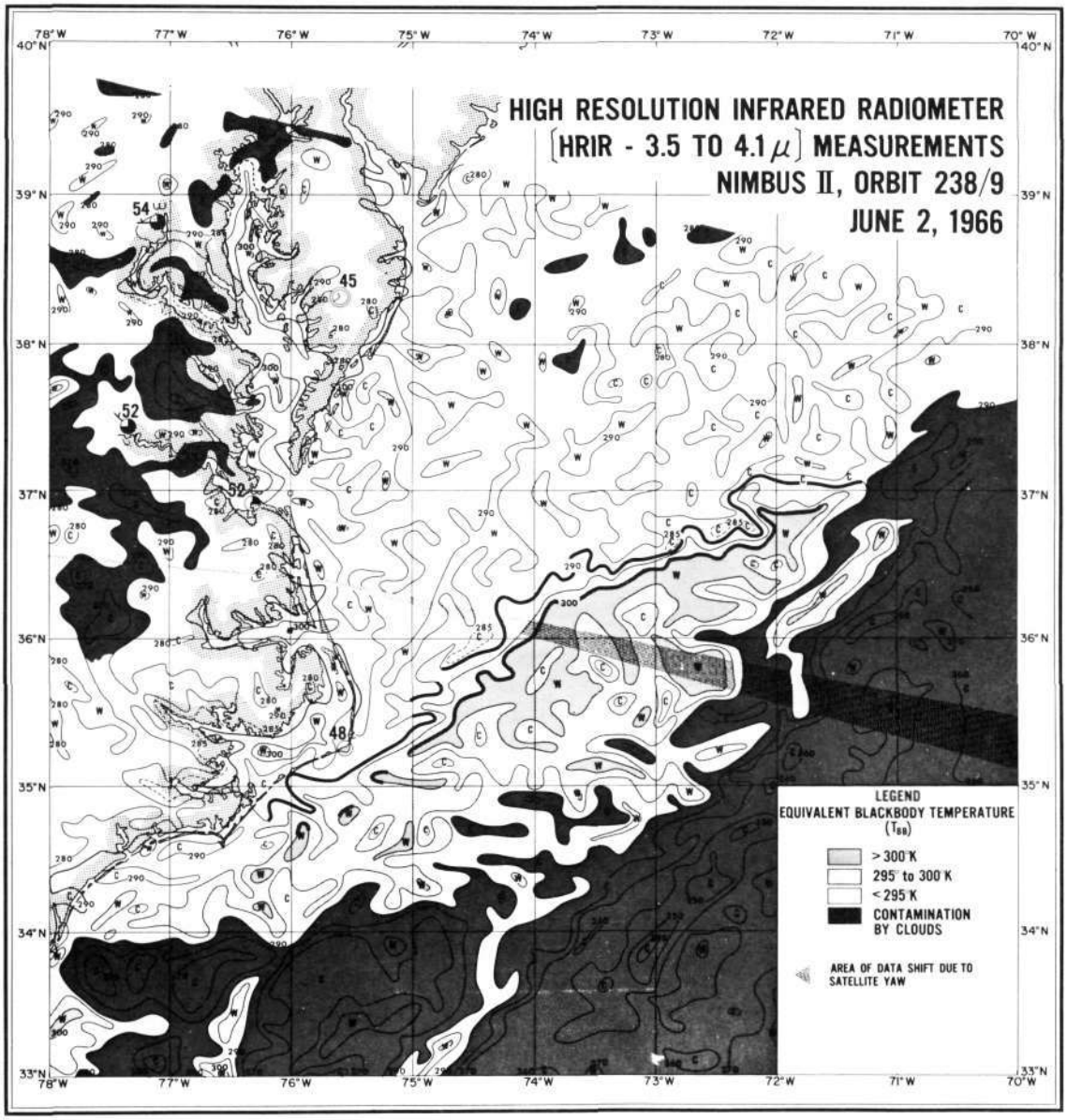

Figure 7. Remote detection of the Gulf Stream boundary by Nimbus II HRIR measurements (After Warnecke, 1968b).

The interpretation of the 15 micron channel measurements in terms of mean temperatures of the lower stratosphere and of stratospheric circulation patterns has been carried out, as it was previously for TIROS VII. The weighting function $d\tau/d$ (log p) for the 14.0-16.0 micron channel of NIMBUS II is shown by the dashed curve in Figure 11. (Because of the narrower spectral interval covered by the NIMBUS III 15 micron channel, its weighting function peaks about 2 km higher than the dashed curve of Figure 11.)

The capability of the NIMBUS II 15 micron data to map stratospheric temperatures on a global scale is shown in Figure 9. The maximum temperature of 240°K is centered over the summer North Pole and the isotherms in the Northern Hemisphere are generally zonal in character with gentle meridional gradients. In the Southern Hemisphere the isotherms are also zonal character but with much stronger meridional gradients in the intense winter polar vortex centered around the South Pole where the minimum temperature of 196°K is found (Warnecke and McCulloch, 1968c).

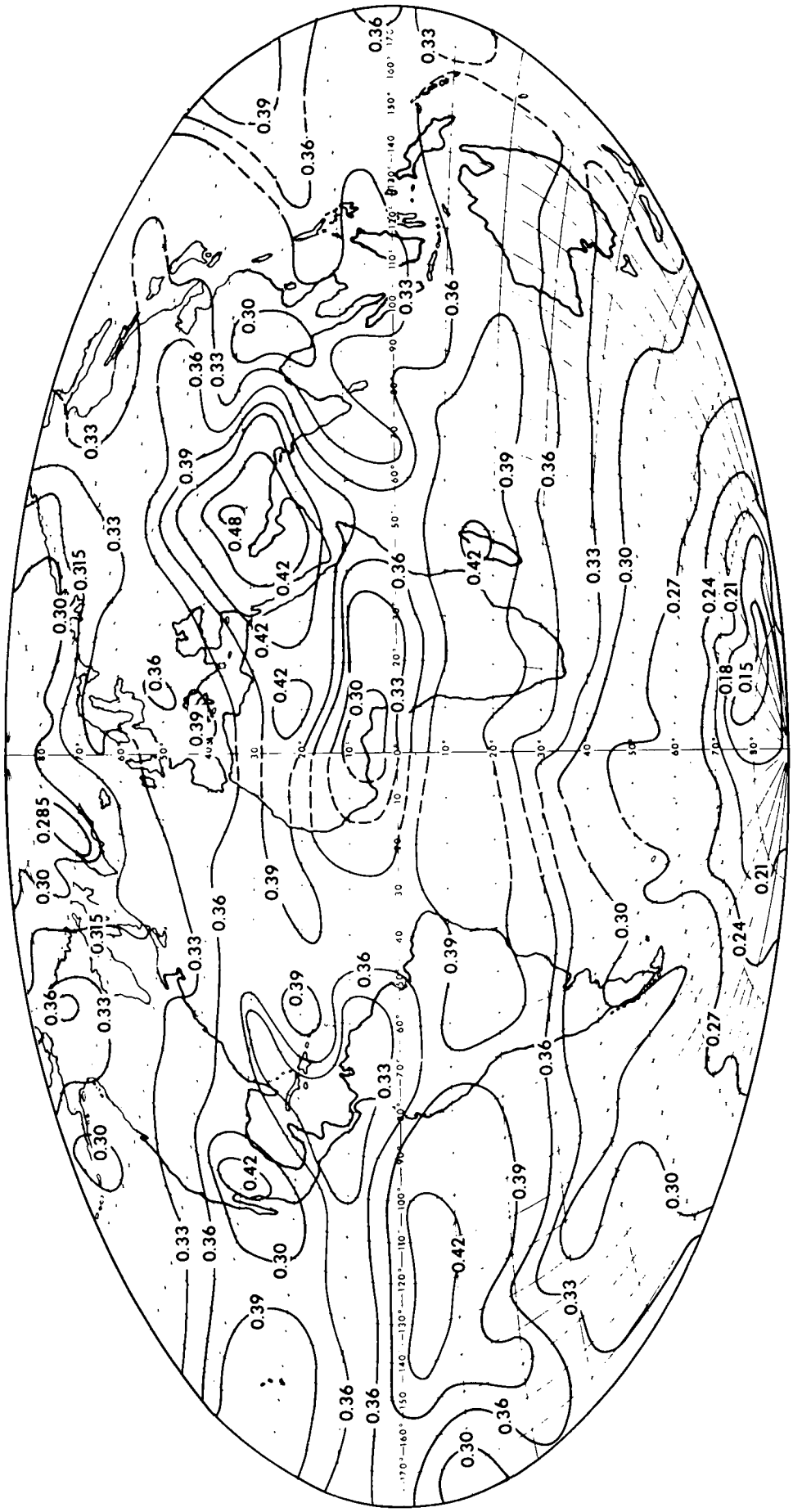

Figure 8. Outgoing total long-wave radiation in cal cm^{-2} min^{-1}, inferred from the Nimbus II 5.0–30.0 micron data and averaged over the period 1–15 June 1966 (After Raschke and Pasternak, 1968).

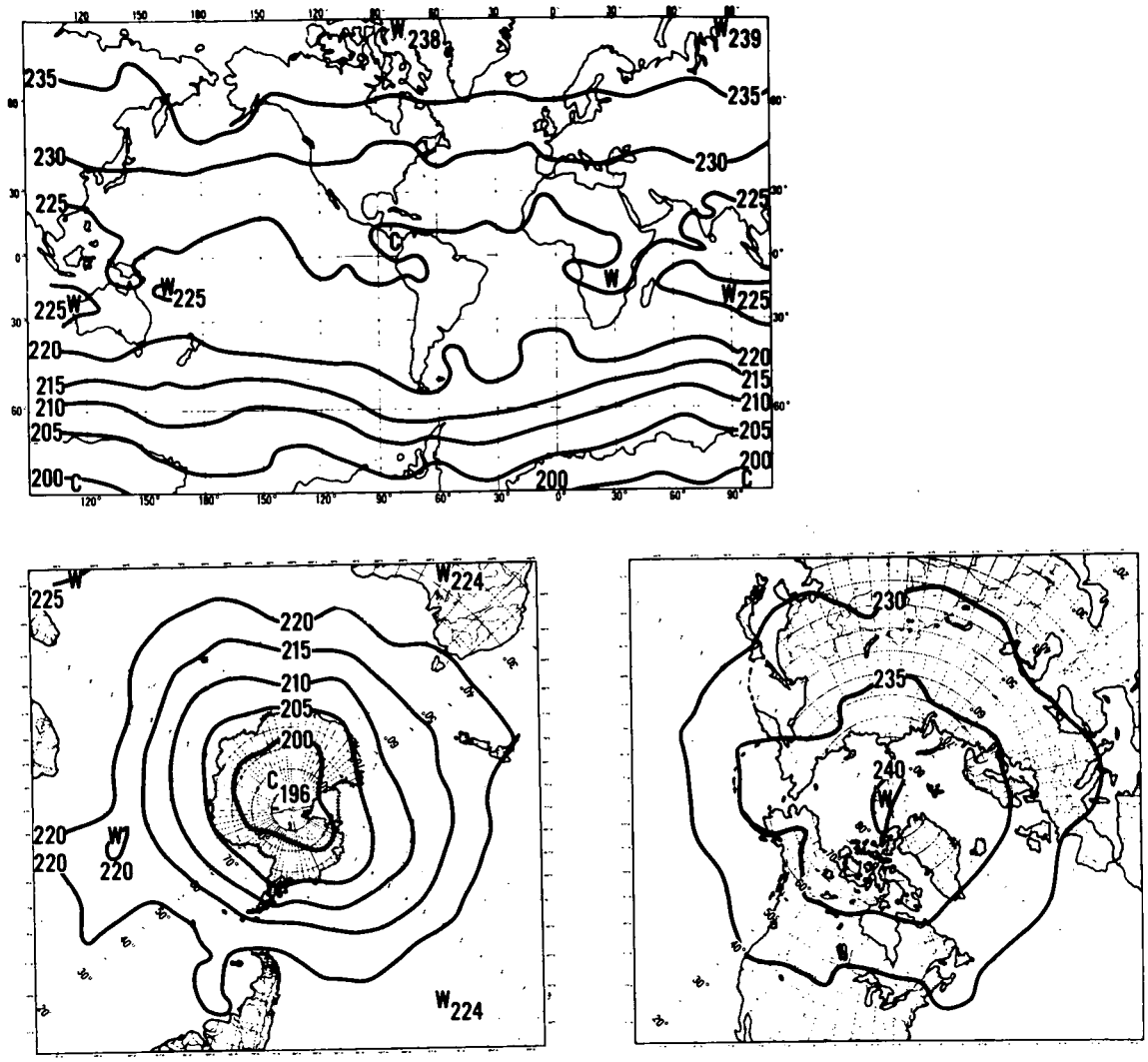

Figure 9. Global stratospheric temperature distribution (°K) from Nimbus II 15 micron measurements on 1 July 1966 (After Warnecke and McCulloch, 1968c).

Figure 10 (top) shows a composite of the cloud picture observed by the 11 micron channel in the belt 30 N - 30 S at local noon on 5 June 1966 except for the two passes near 140 E and 170 E which were obtained at local midnight (Nordberg et al., 1966). Although activity was relatively weak on this day the course of the ITCZ can be followed around the entire globe. The 6.4-6.9 micron water vapor channel observations shown in Figure 10 (bottom) were made simultaneously over the ITCZ. The dark regions on both sides of the cloud zone indicate strong subsidence. Near 140 W the northern band is quite narrow near 30 N over the Pacific and North America and is possibly indicative of the subtropical jet stream. Further east the northern zone of subsidence becomes considerably wider as is the entire southern zone. These wide, dry regions are indicative of the subtropical anticyclones. The warmest (driest) region observed in this channel is in the southern zone near 40 W over eastern Brazil where very strong downward motion can be inferred.

The NIMBUS III MRIR carries a channel sensing in the weakly absorbing 20.0-23.0 micron interval of the rotation band of water vapor (cf. Table 1, No. 5). Radiation sensed by this channel emanates from the lower tropospheric layers, in contrast to the radiation emanating from upper tropospheric layers (i.e., approximately 600 mb to 200 mb) detected

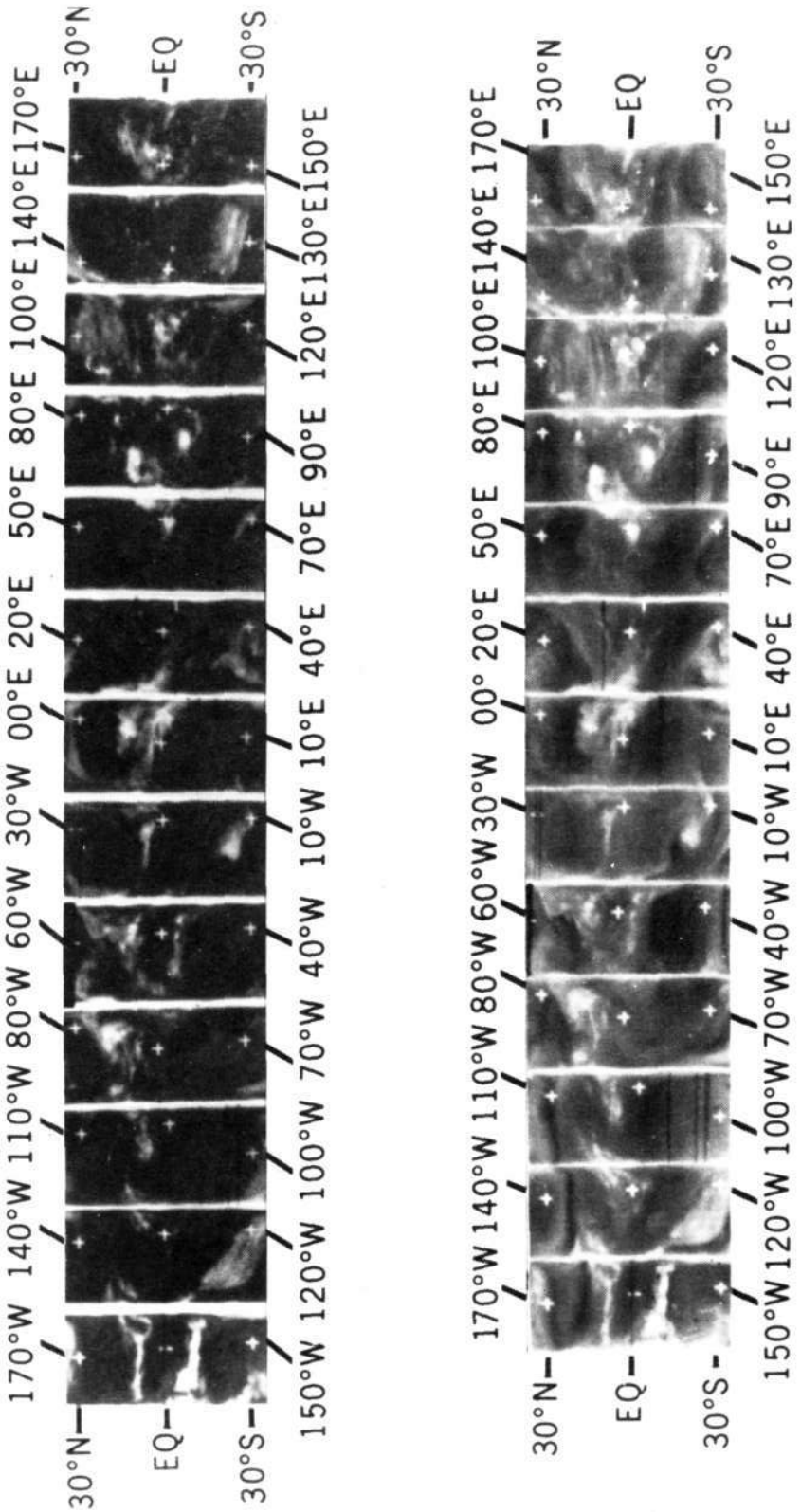

Figure 10. Cloud formations around the globe between 30°N and 30°S observed in the Nimbus II MRIR 10.0–11.0 micron channel (upper band) and 6.4–6.9 micron channel (lower band). Each band is composed of thirteen orbital passes. Reading from right to left, passes 3 through 13 were observed sequentially near local noon on 5 June 1966. Because daytime data over longitudes 130°E to 170°E were not acquired, passes 1 and 2 shown at the right were observed 12 hours later near local midnight (After Nordberg et al., 1966).

by the 6.4-6.9 micron channel, whose spectral interval is centered in a strongly absorbing part of the 6.3 micron band (cf. Figure 1). Although the satellite data are not yet available, it is expected that data from the two water vapor channels will yield additional information on the stratification of vertical motions and moist and dry layers.

3.6 General Discussion of Remote Vertical Sounding

The radiometric instruments discussed heretofore have all sensed radiation in relatively broad spectral intervals and have yielded data having a predominantly two dimensional character, e.g., maps of outgoing radiation originating either at cloud, ground, or water surfaces or within thick regions of the atmosphere. Examples of the latter are maps of mean stratospheric temperatures from the 14.0-16.0 micron channel of the NIMBUS II MRIR. The weighting function for this channel in the 1962 ARDC model atmosphere is shown by the dashed curve in Figure 11. At the half-amplitude points, this curve is more than 20 km thick. When the width of the spectral interval is reduced the shape of the weighting function becomes considerably more peaked and its thickness in the vertical smaller. This sharpening of the weighting function results from the lesser variability of the absorption coefficient over the narrower spectral interval as compared to the broader interval. (Note, however, that in the theoretical limit–for monochromatic radiation – the corresponding width of the weighting function is still about one scale height; cf. Figure 16.)

Five weighting functions for 5 cm^{-1} intervals centered at the indicated wave numbers within the 15 micron carbon dioxide absorption band are shown by the solid curves in Figure 11. The weighting functions located high in the atmosphere correspond to strong absorption whereas those peaking at lower altitudes correspond to weaker absorption.

Although King (1956) originally suggested the possibility of inferring the vertical temperature profile from a nadir scan at one frequency, Kaplan (1959) first suggested the inference of the vertical temperature profile from a frequency scan in the nadir within the 15 micron carbon dioxide band at a spectral resolution of about 5 cm^{-1}. Subsequently a number of authors discussed the problem of remotely inferring vertical atmospheric structure, among them Wark (1961), King (1964), Wark and Fleming (1966), Twomey (1966), Conrath (1967), and Conrath (1968).

The need for remotely sensed vertical profiles of temperature and other meteorological parameters for use in numerical models of the atmosphere during the World Weather Program of the 1970's, including the Global Atmospheric Research Program (GARP), was set forth in the GARP Report of the Stockholm Study Conference (1967). Five different instruments in Table 1 (No.'s 6, 7, 9, 10, and 12) have as a primary purpose the measurement of infrared radiances for inferring such vertical profiles. These will be discussed in turn below.

3.7 Infrared Interferometer Spectrometer (IRIS)

The IRIS is a Michelson interferometer employing a beamsplitter which divides the incoming radiation into two approximately equal components, one directed toward a fixed mirror and the other toward a moving mirror. After reflection from the mirrors, the two beams interfere with each other with a phase proportional to the optical path difference between both beams. The recombined components are then focused onto the

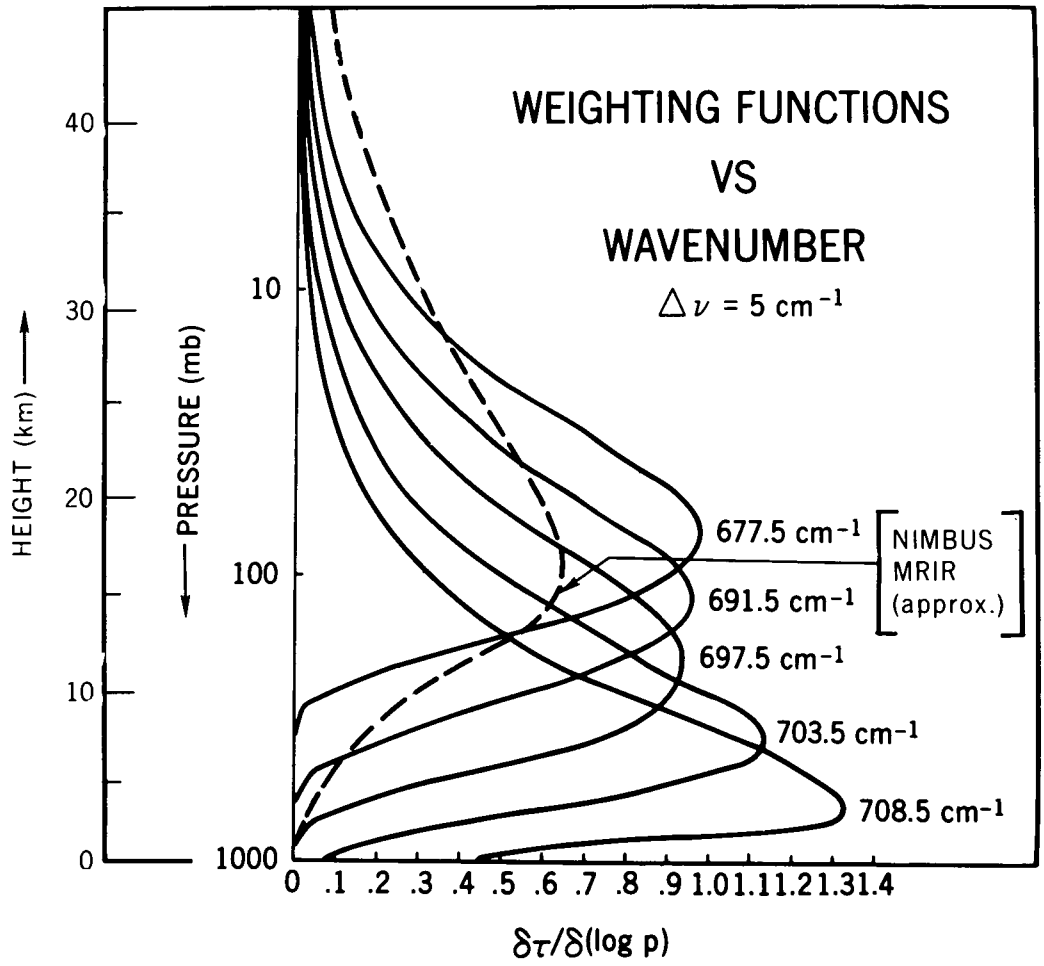

Figure 11. Fifteen micron carbon dioxide absorption band weighting functions (solid lines). The 5 cm^{-1} wide spectral intervals were chosen with mid-points at the indicated wavenumbers (After Conrath, 1968). The weighting function for the 14.0–16.0 micron channel of the Nimbus II MRIR (dashed line) is superimposed on the figure for comparison.

detector where the intensity is recorded as a function of the path difference. For a continuous spectrum, the superposition of many amplitudes of various frequencies takes place. The resultant combined signal is called the interferogram. The spectrum is reconstructed from the interferogram by applying an inverse Fourier transform.

The IRIS views in the nadir direction from the earth-oriented NIMBUS spacecraft. The first IRIS was launched aboard NIMBUS III in May 1968 (cf. Table 1, No. 6a). The design of the instrument has been described by Hanel and Chaney (1966). A description of the instrument is also given in the NIMBUS III User's Guide (1968).

Although at this writing satellite data are not yet available, data have been acquired from a breadboard version of the IRIS flown on a high altitude balloon from Palestine, Texas, on 8 May 1966. The balloon flight and some results from it have been discussed by Chaney, Drayson, and Young (1967). Conrath (1967) also has analyzed the balloon data in terms of inferred temperature and water vapor profiles.

A spectrum obtained with the breadboard version of the IRIS flown at the 7 mb level by the High Altitude Engineering Laboratory of the University of Michigan for the Goddard

Space Flight Center is shown in Figure 12. Included within the spectral interval of this instrument, 500 cm^{-1} (20 microns) to 2000 cm^{-1} (5 microns), are the water vapor absorption band centered at 6.3 microns, the 9.6 micron ozone band, and the 15 micron carbon dioxide band. Hence, information on atmospheric water vapor and ozone should be available from these data, as well as vertical temperature structure from the 15 micron band (Conrath, 1967).

A temperature inversion for the troposphere obtained from IRIS Palestine balloon flight data (such as those of Figure 12) is shown in Figure 13. For comparison data from the 1200 Z and 1800 Z flights of the nearest radiosonde station (Shreveport, Louisiana) are also plotted in Figure 13. At this point it is well to recall that there is some overlapping water vapor absorption in the 15 micron CO_2 band (cf. Figure 1) which should be taken into account if accurate temperature inversions are to be obtained in the lower troposphere. Thus, the water vapor and temperature inversions are essentially coupled. In practice, one can take advantage of the relatively weak dependence of the temperature inversion on water vapor and use a first guess at the humidity profile to obtain a temperature inversion. The resulting temperature profile can be used to do a water vapor inversion in the 6.3 micron band. This procedure can be iterated as many times as necessary (Conrath, 1967).

A two-parameter water vapor mixing ratio inversion of IRIS data from the Palestine balloon flight is shown in Figure 14. Radiosonde data taken the same day at Shreveport are included in the figure (Conrath, 1967). In this trial water vapor inversion, the average temperatures from the two radiosonde runs furnished the necessary knowledge of the temperature profile. In actual operations using satellite data, this knowledge would be obtained from an inversion of 15 micron data, such as that performed to yield the profile of Figure 13.

Conrath (1967) also briefly discussed the problems attending the inversion of spectra in the 9.6 micron band to infer the vertical distribution of ozone. He points out that the atmosphere is not optically thick even in the strongest part of the 9.6 micron band and that the bulk of the ozone in a typical distribution is located at heights where the pressure broadening of individual lines is low. Weighting functions calculated by Bolle (1967) show widths greater than the characteristic heights over which the ozone concentration varies. Conrath (1967) concludes that it will be difficult to extract information on the vertical ozone distribution in any detail with IRIS data.

The second IRIS is scheduled to fly on NIMBUS D (cf. Table 1, No. 6b). It will be a somewhat modified verision of the first instrument, e.g., the spectral coverage will be shifted to longer wavelengths to include the rotation band of water vapor, and both the spectral and spatial resolutions will be increased (Hanel, 1968).

3.8 Satellite Infrared Spectrometer (SIRS)

The SIRS is a modified Fastie-Ebert grating spectrometer. The radiant energy is detected behind each exit slit by a wedge-immersed thermistor bolometer. Design considerations leading to the satellite version have been discussed by Dreyfus and Hilleary (1962) and Hilleary, et al. (1966).

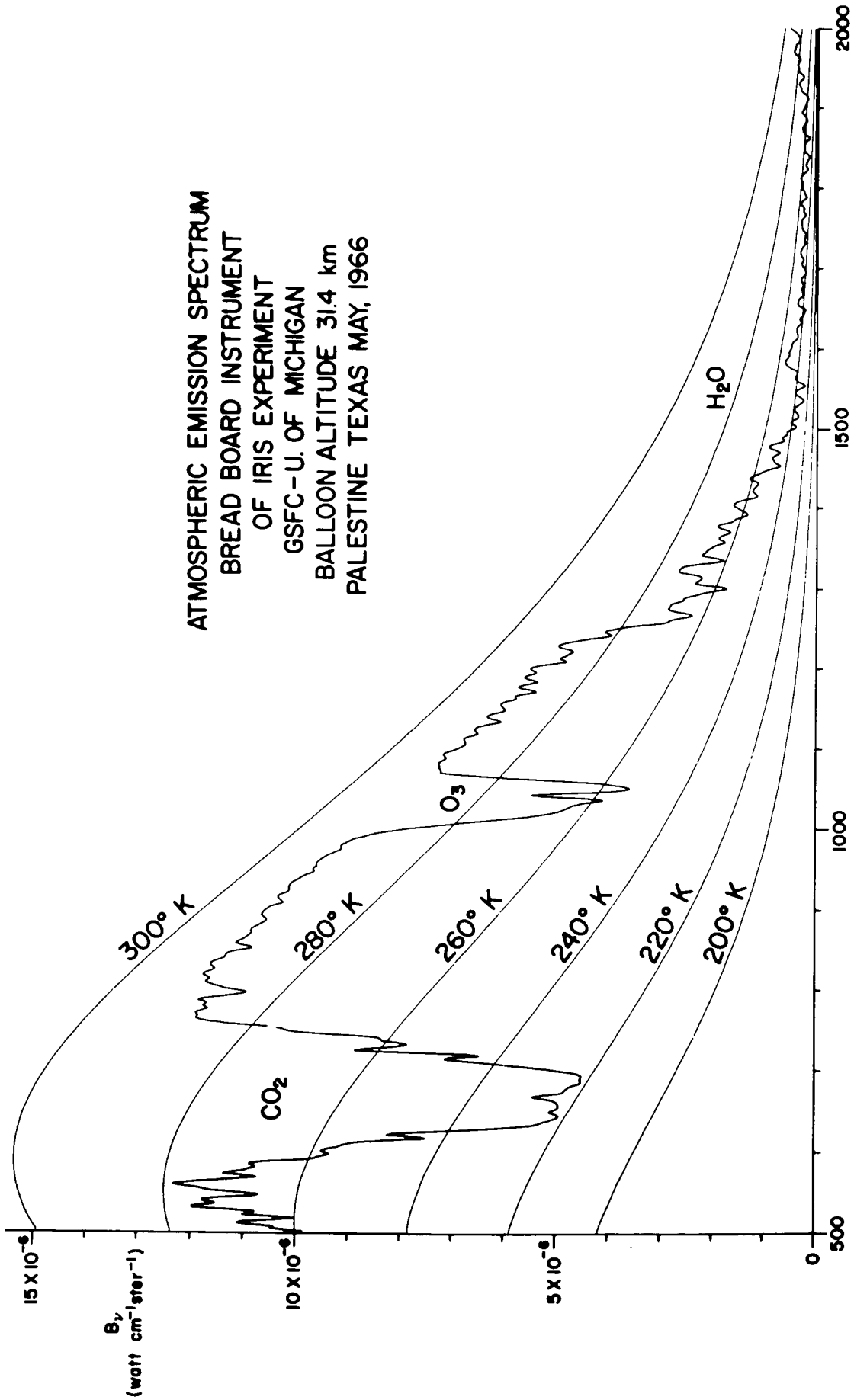

Figure 12. Atmospheric spectrum acquired with a breadboard version of an IRIS instrument in a balloon flight, 8 May 1966, from Palestine, Texas (After Conrath, 1967).

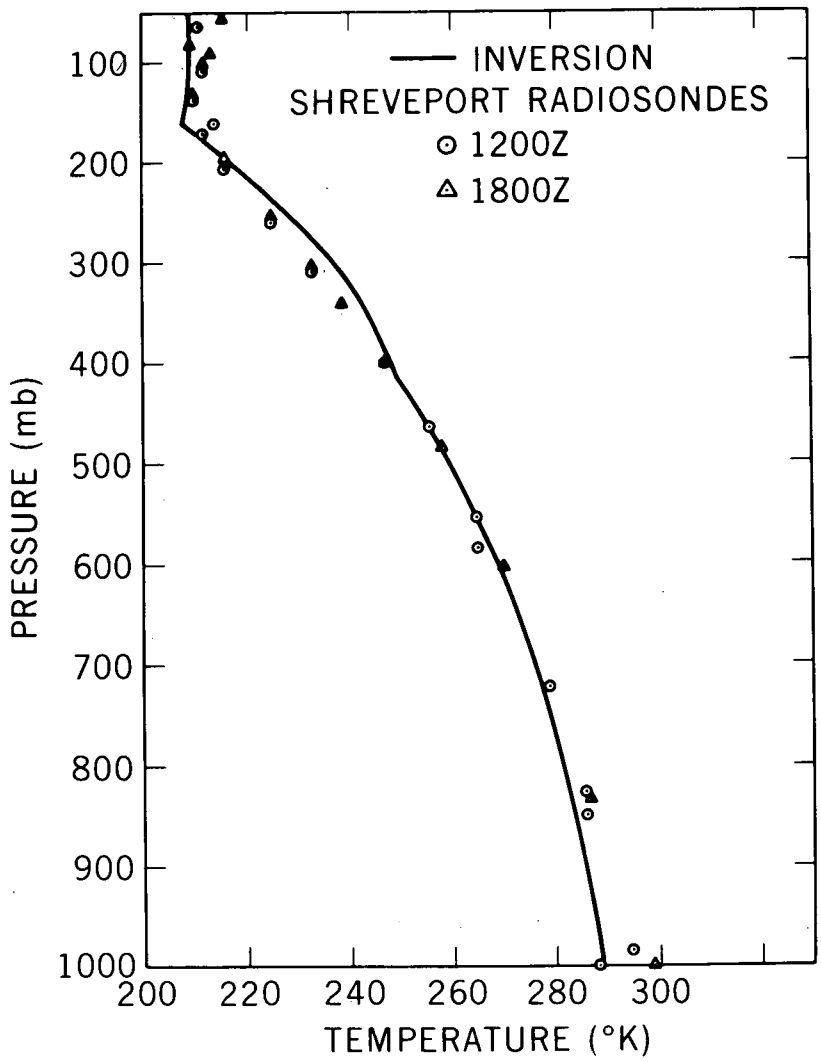

Figure 13. Tropospheric temperature inversion from IRIS data in the 15 micron carbon dioxide band. The data were acquired during the balloon flight on 8 May 1966 from Palestine, Texas (After Conrath, 1967).

The SIRS views in the nadir direction from the NIMBUS spacecraft. The first SIRS was launched aboard NIMBUS III in May 1968 (cf. Table 1, No. 7a). A description of the flight instrument and a discussion of the experiment are given in the NIMBUS III Users' Guide (1968). The mid-points of the 5 cm^{-1} wide spectral intervals sensed over the 15 micron carbon dioxide band are the following: 669.0 cm^{-1}, 677.5 cm^{-1}, 692.0 cm^{-1}, 669.0 cm^{-1}, 706.0 cm^{-1}, 714.0 cm^{-1}, and 750.0 cm^{-1}. The eighth channel senses radiation in the atmospheric window, centered at 899.0 cm^{-1}.

Although at this writing satellite data are not yet available, analyses of data from ground-based instruments similar to SIRS have been carried out by James (1967) and Wolk and Van Cleef (1967), and results from balloon-borne versions of SIRS have been reported by Hilleary, et al. (1965) and Wark, et al. (1967). Figure 15 shows a temperature profile in clear skies deduced from data from a spectrometer flown on a balloon from Palestine, Texas, on 11 September 1964.

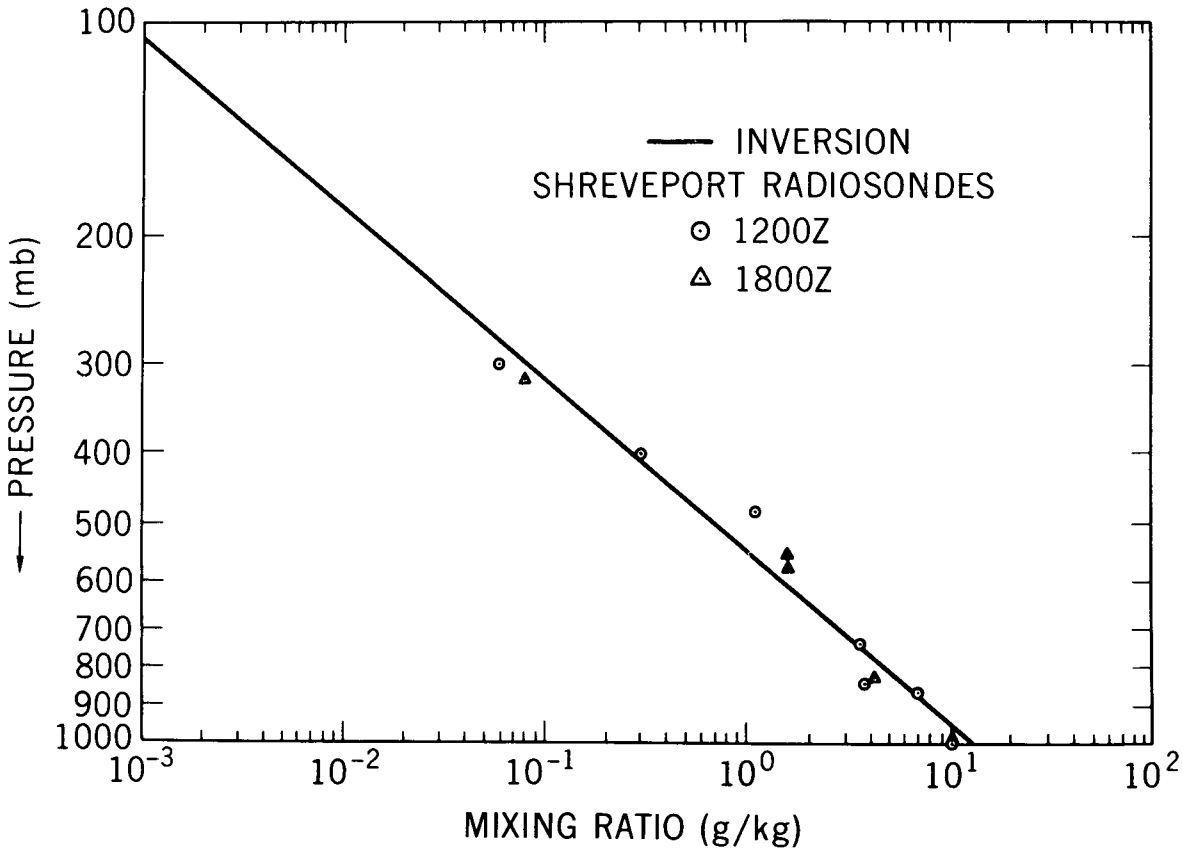

Figure 14. Two-parameter water vapor mixing ratio inversion from IRIS data in the 6.3 micron band. The data were acquired during the balloon flight on 8 May 1966 from Palestine, Texas (After Conrath 1967).

The second SIRS is scheduled to fly on NIMBUS D (cf. Table 1, No. 7b). It will be an augmented version of the first instrument, viz., in addition to the eight channels of the first SIRS, the second will have six channels sensing in 5 cm^{-1} wide spectral intervals over the rotation band of water vapor. The mid points of these intervals are the following: 280.0 cm^{-1}, 302.5 cm^{-1}, 290.5 cm^{-1}, 424.5 cm^{-1}, 488.0 cm^{-1}, and 531.5 cm^{-1}. The purpose of adding the six additional channels is to acquire data for deducing water vapor (as well as temperature) profiles. Another significant modification in the NIMBUS D SIRS is a step-scanning feature by which the optical axis of the spectrometer will view at a nadir angle of 25°-to-39° to the left for one minute, followed by viewing in the nadir direction for a second minute, followed by viewing at a nadir angle of 25°-to -39° to the right for a third minute. This cycle will be repeated continuously, and the side-viewing nadir angles will be programmed to vary from 39° (at the equator) to 25° at high latitudes in order to effect an optimum grid spacing for computer input data for numerical modelling (Wark, 1968).

3.9 ITOS High Resolution Radiometer

A High Resolution Radiometer is being developed for the second generation operational meteorological satellite system, also called the Improved TIROS Operational Satellite System–ITOS (Operational Satellites Office, 1968). Selected characteristics of this radiometer are given in Table 1, No. 8. This instrument will be mounted on the earth-oriented, three-axis-stabilized platform of the gyro-magnetically controlled ITOS

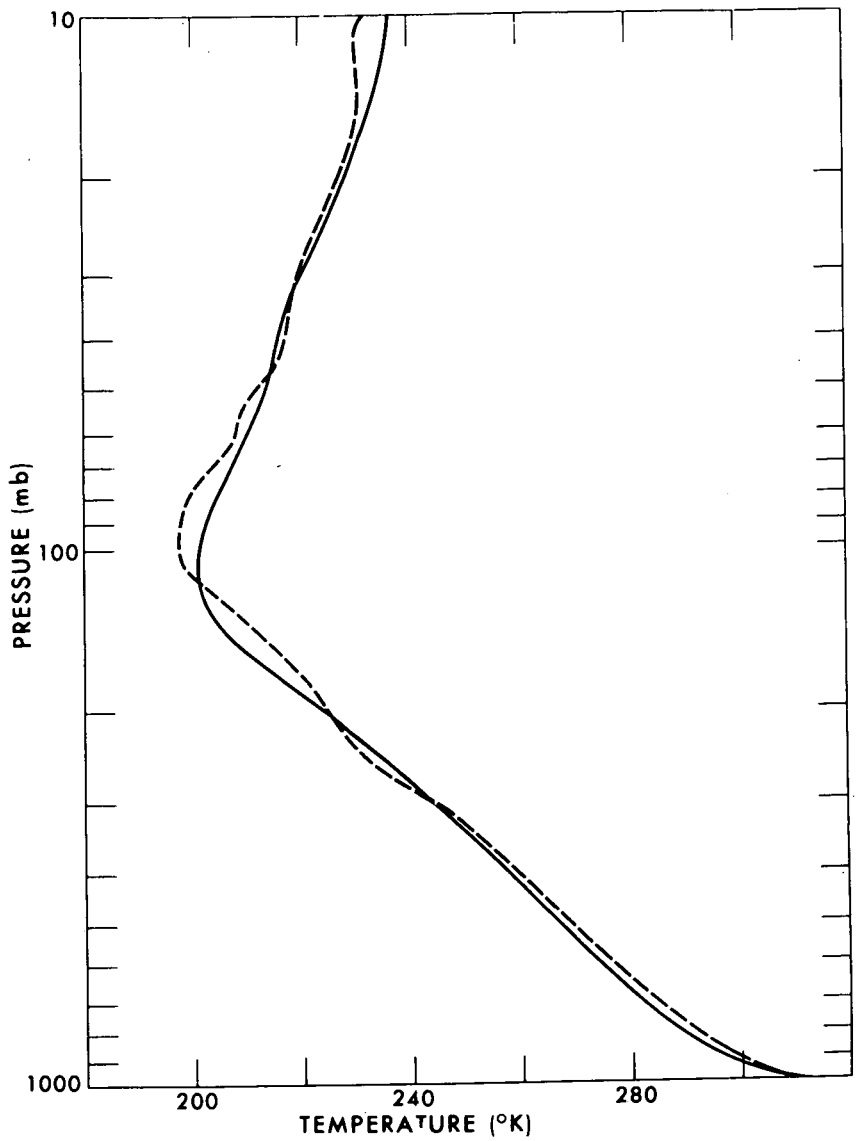

Figure 15. Deduced temperature profile in clear skies from data in the 15 micron carbon dioxide band acquired at 7:57 a.m. CST by a balloon borne version of SIRS (solid line). The balloon was launched to an altitude of 100,000 ft. on 11 September 1964 from Palestine, Texas. The dashed line is the noon CST profile from the Fort Worth radiosonde (After Wark et al., 1967).

vehicle and, therefore, will have a primary mirror scanning transverse to the spacecraft motion much like the NIMBUS HRIR and MRIR. The ITOS High Resolution Radiometer, although essentially duplicating spectrally two of the channels of the TIROS and NIMBUS Medium Resolution Radiometers, will have the advantage of a much higher spatial resolution (even somewhat higher than that of the NIMBUS HRIR). Hence, the quality of the photo-images should approach that of television cameras. Also, the probability in areas of partial cloud cover of either cloud elements or land or water surfaces completely filling the instantaneous field of view of the instrument will be vastly increased. Obviously under these conditions the interpretation of the data in terms of cloud top and land and sea surface temperatures will be more meaningful. Although the ITOS Radiometer is improved only slightly over the NIMBUS HRIR in spatial

resolution, it will be a decided improvement over the latter by being able to measure surface temperatures in the 10.5-12.5 micron interval equally well both day and night, and by being able to determine whether an area is cloud-free in the daytime by means of the synchronized visible channel measurements. Thus satellite measurements of land and sea surface temperatures and temperature gradients will be of increased accuracy and, consequently, increased usefulness in such applications as meteorology, oceanography, geomorphology, etc.

In addition to the stored-data mode of operation, the 10.5-12.5 micron channel of the ITOS High Resolution Radiometer will be adapted to the Automatic Picture Transmission (APT) system, constituting a Direct Readout of Infrared (DRIR) system. The DRIR system will operate throughout the entire orbit, reading out infrared imagery to APT stations all over the world in the nighttime and in the daytime as well (when the infrared data will be interleaved with the Standard APT pictures) (Operational Satellites Office, 1968).

3.10 Selective Chopper Radiometer (SCR)

A Selective Chopper Radiometer (SCR) is being developed to fly on NIMBUS D for the purpose of atmospheric temperature sounding (cf. Table 1, No. 9). The SCR will view in the nadir direction from the NIMBUS spacecraft. The basic optical system consists of a movable mirror, simple flapping choppers arranged in opposed pairs, germanium lens optical systems, interference filters, and a light pipe to condense radiation onto a thermistor bolometer detector. A description of the radiometer and a discussion of the experiment have been given by Peckham, et al. (1966) and by the Oxford Reading Group (1966).

A distinctive feature of the SCR is the use of very narrow band interference filters combined with CO_2 selective chopping and absorption cells to lessen the effective variation of the absorption coefficient over the spectral interval and, hence, to improve the height resolution of the weighting function and to make possible the measuring of the vertical temperature structure from the ground (or highest cloud top) to 50 km.

In connection with the channels associated with the two weighting functions peaking at the higher altitudes, a technique of selective chopping by CO_2 is used. The incoming radiation beam is switched between a cell containing CO_2 and a nearly-empty cell containing only a small amount of CO_2 at very low pressure. This technique has the effect of sensing only the radiation near the strongly-absorbing line centers (except the very centers of the lines, which are eliminated by the nearly-empty cell, thus further sharpening the weighting functions).

For the channels associated with the four weighting functions peaking at the lower altitudes, a single absorption cell is used to absorb out the line centers. This technique has the effect of sensing only the radiation toward the weakly-absorbing wings of the lines. A weighting function applying to a single absorption cell (C) is compared in Figure 16 with weighting functions applying to monochromatic radiation (M) and to a spectrometer (such as IRIS and SIRS) sensing over a spectral interval including many individual lines (S). An Elsasser band model was used in carrying out the calculations for Figure 16. It is seen that the absorbing cell weighting function differs very little from the monochromatic weighting function and is considerably sharper than the

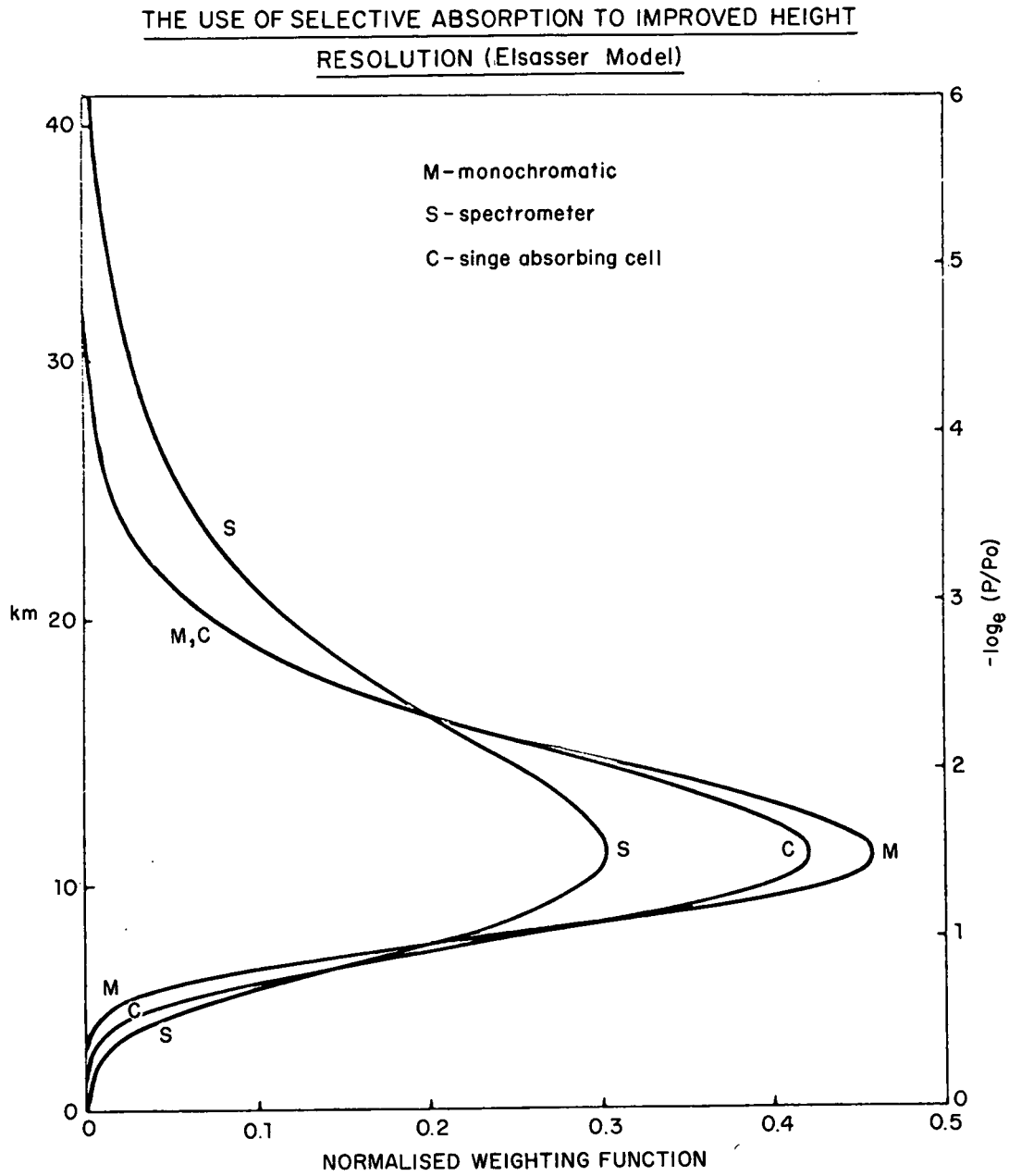

Figure 16. A comparison of weighting functions applying to monochromatic radiation (M), a spectrometer (S), and the single absorbing cell (C) of the Selective Chopper Radiometer (After Oxford-Reading Group, 1966).

spectrometer weighting function. One of the six channels of the SCR is switchable to 11 microns to provide surface temperature data for use in the inversion analysis.

A successful balloon flight of the SCR was made at 0300 hours on 9 June 1966. The balloon reached a height of 35 km over the southern counties of England. Satisfactory signals were received and indicated proper operation of the radiometer. The results of this flight and a complete discussion of the experiment and the instrument will soon be published in a series of papers in the open literature (Williamson, 1968).

3.11 Filter Wedge Spectrometer (FWS)

A Filter Wedge Spectrometer (FWS) is being developed to fly on NIMBUS D. Selected characteristics of the FWS are given in Table 1, No. 10. The FWS will view in the nadir direction from the NIMBUS spacecraft. The heart of the instrument is an interference filter wedge, consisting of a pair of halves of two filters—one covering the range 1.2-2.4 microns, and the other the range 3.2-6.4 microns. The assembly of two halves is necessary since present technology allows only one octave of spectrum to be covered on one disc, the same octave being covered twice in one 360° rotation (Hovis, Kley, and Strange, 1967). The instrument will utilize a lead selenide detector, radiatively cooled to 160°K.

The FWS will obtain continuous spectra at a resolution of $\lambda/\Delta\lambda = 100$ of reflected solar and emitted thermal radiation from the earth and atmosphere in the two spectral intervals stated above. Three specific applications are identified. The first is to test the feasibility of determining whether a cloud is composed of ice crystals (cirrus) or water droplets. Blau, et al. (1966) reported among other features a characteristic minimum at 2.0 microns, observed in spectra of ice clouds taken from a high altitude aircraft. This minimum is absent in spectra of liquid-water clouds. In a series of flights of the NASA Convair-990 research aircraft in the spring of 1966, reflection and emission spectra were obtained by an aircraft version of the FWS over many types of clouds and other natural surfaces. The characteristic minimum at 2.0 microns was observed over cirrus clouds while over water clouds it was absent. This feature is evident in the three sequential spectra over cirrus clouds shown in Figure 17.

The second application is to infer the vertical temperature profile from spectral measurements in the 4.3 micron band of carbon dioxide in much the same manner as the temperature profile is inferred from measurements in the 15 micron band. A temperature profile of the atmosphere, determined from an analysis of measurements in the region of the 4.3 micron CO_2 band made by a balloon-borne grating spectrometer, and the techniques used and some of the problems encountered have been discussed by Shaw, McClatchey, and Schaper (1967).

The third application is to infer the water vapor profile from measurements in the region of the 6.3 micron band, having already determined the temperature profile. As mentioned in the discussion of the IRIS instrument, Conrath (1967) has investigated the problem of remotely inferring water vapor profiles.

3.12 Temperature Humidity Infrared Radiometer (THIR)

A Temperature Humidity Infrared Radiometer (THIR) is being developed to fly on NIMBUS D. Selected characteristics of the THIR are given in Table 1, No. 11. The scanner design uses an elliptically shaped plane scan mirror set at an angle of 45° (similar to that of the NIMBUS HRIR and MRIR and of the ITOS High Resolution Radiometer) and primary optics which are common to both channels. The two channels are separated by means of a dichroic beam splitter (McCulloch, 1968).

A 10.5-12.5 micron channel having a linear resolution at the subsatellite point of 7-to-8 km will be flown on TIROS M (cf. Table 1, No. 8); hence a test of the feasibility of a day-night operational cloud mapping instrument with high spatial resolution will have been accomplished prior to NIMBUS D. Therefore the purpose of this channel will largely be to provide supporting data for all scientific experiments on the spacecraft.

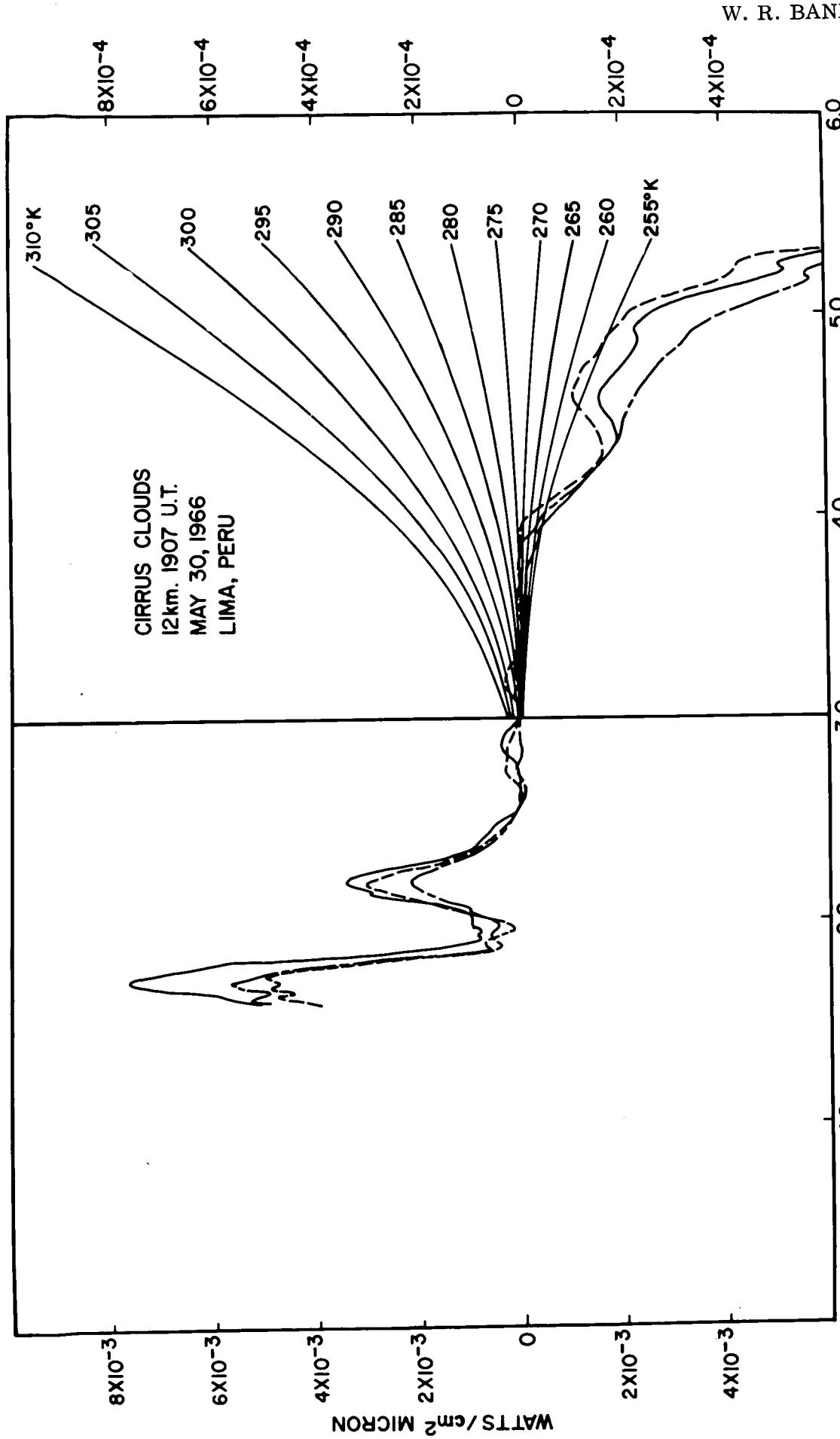

Figure 17. Three sequential spectra from a Filter Wedge Spectrometer on a jet aircraft over cirrus clouds, showing a characteristic minimum at 2.0 microns. The ordinate to the right of 3.0 microns is expanded ten-fold and blackbody curves are drawn for every 5°K (After Hovis and Tobin, 1967).

The new and distinctive feature of the THIR is the 6.5-7.0 micron water vapor channel having better than twice the linear resolution of the comparable channel of the NIMBUS II and III MRIR. The inclusion of a water vapor channel will permit further studies at improved spatial resolution of the synoptic significance of the moisture patterns first detected in the 6.4-6.9 micron data of NIMBUS II as typified by Figure 10. Of particular interest will be the possibility of using the 6.5-7.0μ data to trace air mass boundaries, vertical motions, and possibly the course of jet streams.

3.13 ITOS Vertical Temperature Profile Radiometer (VTPR)

A Vertical Temperature Profile Radiometer (VTPR) is being developed for the Improved TIROS Operational Satellite System-ITOS (Operational Satellites Office, 1968). Selected characteristics of this radiometer are given in Table 1, No. 12. The VTPR will view in the nadir direction from the earth-oriented platform of the ITOS vehicle. A final determination of the wave numbers at the mid-points of the eight channels has not been made, but there will probably be six channels ranging from about 669.0 cm^{-1} to 750.0 cm^{-1} in the 15 micron CO_2 band, one channel sensing at about 532 cm^{-1} in the rotation band of water vapor, and one channel sensing in the atmospheric window at 899 cm^{-1}. The spectral resolution for all channels will be about 5 cm^{-1}. This instrument is intended solely for the probing of the temperature profile from operational satellites, and it takes advantage of the latest advances in technology. For example, it utilizes one set of optics and one thermistor bolometer with a cone optic behind a filter wheel. The weight and power requirements of the instrument are notably small (about 10 pounds and 2 watts) compared to those of earlier instruments designed for vertical temperature probing (e.g., SIRS: 92 pounds and 20 watts, or IRIS: 28 pounds and 12 watts).

3.14 ITOS Very High Resolution Radiometer (VHRR)

A Very High Resolution Radiometer (VHRR) is being developed for the Improved TIROS Operational Satellite System-ITOS (Operational Satellites Office, 1968). Selected characteristics of this radiometer are given in Table 1, No. 13. The linear resolution on the ground of this instrument represents an order-of-magnitude improvement over that of the NIMBUS HRIR and ITOS High Resolution Radiometer and a nearly two-orders-of-magnitude improvement over that of the TIROS and NIMBUS Medium Resolution Radiometers (cf. Table 1). As such, the resolution of the VHRR is comparable to that of television systems currently flown on meteolorogical satellites. To achieve this resulution a mercury-cadmium-telluride detector, radiatively-cooled in two stages to 80°K will be used. But with the capability of the 10.5-12.5 micron channel to make measurements day and night, while the 0.52-0.73 micron channel is also making measurements in the daytime, the bit rate of the instrument far exceeds the capacity of any presently available tape recorder system. Therefore, the present plans are to read out the data directly (possibly via a relay geosynchronous satellite). Other possibilities include recording the VHRR data over only a portion of the orbit (a portion determined to be of high interest from other instruments) or recording a degraded form of the data over the entire orbit.

The applications of the data will be similar to those of the other scanning radiometers sensing in similar spectral intervals except that the much higher resolution will permit the study of smaller-scale phenomena such as the three-dimensional structure of cloud patterns and frontal systems and the possible distribution of multiple "hot tower" cumulus cells in hurricanes and typhoons.

3.15 Very High Resolution Radiometer for Geosynchronous Altitude

All of the radiometric instruments discussed to this point have been designed for single-satellite systems which permit observations of a given location on earth approximately once every twelve hours. However, there are many meteorological phenomena which have characteristic time periods much shorter than twelve hours, e.g., the development of hurricanes, typhoons, and other types of storms (most notably tornadoes whose whole life cycle can extend over only tens of minutes); the change in the motion of storm systems; and the change in identifiable cloud features which over a shorter period of time might serve as atmospheric tracers to determine winds and other kinematic properties of the atmosphere. The spin scan cloud cameras recently flown on the ATS-1 and ATS-3 satellites in geosynchronous orbits have indicated that a wealth of new information exists both because of the planetary view from the geosynchronous distance of 35,800 km and because of the time-lapse characteristic of the ATS pictures taken every twenty minutes. The possibility of determining flow patterns and wind velocities, and of studying the buildup and decay of short-lived systems and the interactions between hemispheres across the equator have been indicated (McQuain, 1967; Warnecke and Sunderlin, 1968d).

A Very High Resolution Radiometer for Geosynchronous Altitude has been proposed for future flight. Selected characteristics of this radiometer are given in Table 1, No. 14. The design of the proposed radiometer and other characteristics of the experiment have been discussed by Goldberg (1968). The radiometer has several important advantages over a camera that senses visible radiation. First the familiar "full earth" pictures made with the ATS cameras can be taken only during a small fraction of the day, while other pictures taken during the 24 hour period show varying smaller portions of the earth, depending on the location of the terminator. However, the radiometer system will take "full earth" pictures on every frame, independent of the position of the terminator.

Figure 18 attempts to illustrate how a radiometer "picture" of the earth at night (or in the daytime) might look. The model of the earth shown in Figure 18 was constructed by pasting orbital strips of NIMBUS II nighttime HRIR data in correct geographic sequence on a 10-inch-diameter globe (Warnecke, 1968b). The coldest areas are shaded white and the warmest are black with intermediate shades in between. Clearly identifiable are high white (cold) cloud patterns and dark (warm) ocean areas through clear skies. The Australian continent stands out in light shading (colder than the surrounding ocean at night) in the lower left part of the picture. There are marked distortions at the edges of the orbital strips because of the relatively low height of the NIMBUS satellite, but these do not seriously impair the general impression of a high resolution view of the earth in the spectral interval 10.5-12.5 microns from a geosynchronous satellite.

Another advantage of the radiometer over a camera is the capability of temperature measurement. Cloud top altitudes can be inferred from cloud top temperatures, and sea surface temperature variations such as those due to the Gulf Stream can be observed in cloud free regions. Also winds inferred from time-lapse movements of cloud patterns can be located approximately in height because of the temperature measuring capability of the radiometer. The importance of this type of experiment was set forth in the GARP Report of the Stockholm Study Conference (1967).

REFERENCES

Allison, Lewis J., Thomas I. Gray, Jr., and Guenter Warnecke, 1964: A Quasi-Global Presentation of TIROS III Radiation Data. Special Publication SP-53, NASA, Washington, D.C., 23 pp.

Allison, Lewis J., George W. Nicholas, and James S. Kennedy, 1966a: Examples of the Meteorological Capability of the High Resolution Infrared Radiometer on the Nimbus I Satellite. Jour. Appl. Meteor., 5, 314-333.

Allison, Lewis J. and Harold P. Thompson, 1966b: TIROS VII Infrared Radiation Coverage of the 1963 Atlantic Hurricane Season with Supporting Television and Conventional Meteorological Data. Technical Note TN D-3127, NASA, Washington, D.C., 48 pp.

Allison, Lewis J. and Guenter Warnecke, 1966c: The Interpretation of TIROS Radiation Data for Practical Use in Synoptic Weather Analysis. Beiträge zur Physik der Atmos., 39, 165-181.

Allison, Lewis J. and Guenter Warnecke, 1967: A Synoptic World Weather Analysis of TIROS VII Radiation Data. Technical Note TN D-3787, NASA, Washington, D.C., 34 pp.

Bandeen, W. R., R. A. Hanel, J. Licht, R. A. Stampfl, and W. G. Stroud, 1961: Infrared and Reflected Solar Radiation Measurements from the TIROS II Meteorological Satellite. Jour. Geophys. Res., 66, 3169-3185.

Bandeen, W. R., B. J. Conrath, and R. A. Hanel, 1963a: Experimental Confirmation from the TIROS VII Meteorological Satellite of the Theoretically Calculated Radiance of the Earth Within the 15-Micron Band of Carbon Dioxide. Jour. Atmos. Sci., 20, 609-614.

Bandeen, W. R., B. J. Conrath, W. Nordberg, and H. P. Thompson, 1963b. A Radiation View of Hurricane Anna from the TIROS III Meteorological Satellite, pp. 224-233 in Proceedings of the First International Symposium on Rocket and Satellite Meteorology, ed. H. Wexler and J. E. Caskey, Jr., North-Holland Publishing Co., Amsterdam, 440 pp.

Bandeen, W. R., V. Kunde, W. Nordberg, and H. P. Thompson, 1964: TIROS III Meteorological Satellite Radiation Observations of a Tropical Hurricane. Tellus, XVI, 481-502.

Bandeen, W. R., M. Halev, and I. Strange, 1965: A Radiation Climatology in the Visible and Infrared from the TIROS Meteorological Satellites. Technical Note TN D-2534, NASA, Washington, D.C., 30 pp.

Bandeen, W. R., 1966: Atmospheric Water Vapor Content from Satellite Radiation Measurements, pp. 229-249, in Satellite Data in Meteorological Research, NCAR-TN-11, ed. H. M. E. Van de Boogaard. National Center for Atmospheric Research, Boulder, Colorado, 349 pp.

Bartko, Frank, Virgil Kunde, Clarence Catoe, and Musa Halev, 1964: The TIROS Low Resolution Radiometer. Technical Note TN D-614, NASA, Washington, D.C., 34 pp.

Belmont, A. D., G. W. Nicholas, and W. C. Shen, 1968: Comparison of 15-μ TIROS VII Data with Radiosonde Temperatures. Jour. Appl. Meteor., 7, 284-289.

Blau, Henry H., Jr., Ronald P. Espinola, and Edward C. Reifenstein, III, 1966: Near Infrared Scattering by Sunlit Terrestrial Clouds. Appl. Optics, 5, 555-564.

Bolle, H. J., 1967: Infrarotspektroskopie als Hilfsmittel und Gegenstand meteorologischer und planetarischer Forschung. Meteorologisches Institut der Ludwig-Maximilians - Universität München Forschungsbericht W 67-17 (July).

Buettner, Konrad J. K. and Clifford D. Kern, 1963: Infrared Emissivity of the Sahara from TIROS Data. Science, 142 (Nov. 8), 671.

Chaney, L. W., S. R. Drayson, and C. Young, 1967: Fourier Transform Spectrometer-Radiative Measurements and Temperature Inversion. Applied Optics, 6, 347-349.

Conrath, Barney J., 1967: Remote Sensing of Atmospheric Water Vapor and Ozone Using Interferometry, pp. 277-296 in Proceedings of the Specialists Conference on Molecular Radiation and Its Application to Diagnostic Techniques, Marshall Space Flight Center, 5-6 October 1967. Document TM X-53711, ed. R. Goulard, NASA, Marshall Space Flight Center, 489 pp.

Conrath, B. J., 1968: Inverse Problems in Radiative Transfer: A Review, pp. 339-360 in Proceedings of the XVIII International Astronautical Congress, Belgrade, October 1967. (Also available as Doc. X-622-67-57, NASA Goddard Space Flight Center.)

Davis, Paul A. 1965: TIROS III Radiation Measurements and Some Diabatic Properties of the Atmosphere. Mo. Weather Rev., 93, 535-545.

Dreyfus, M. G. and D. T. Hilleary, 1962: Satellite Infrared Spectrometer. Aerospace Engrg., February, 42-45.

Foshee, L. L., I. L. Goldberg, and C. E. Catoe, 1965: The High Resolution Infrared Radiometer (HRIR) Experiment, pp. 13-22 in Observations from the Nimbus I Meteorological Satellite. Special Publication SP-89, NASA, Washington, D.C., 90 pp.

Fritz, Sigmund and Jay S. Winston, 1962: Synoptic Use of Radiation Measurements from Satellite TIROS II. Mo. Weather Rev., 90, 1-9.

Fritz, Sigmund, 1963: The Diurnal Variation of Ground Temperature as Measured from TIROS II. Jour. Appl. Meteor., 2, 645-648.

Fritz, S. and P. Krishna Rao, 1967: On the Infrared Transmission Through Cirrus Clouds and the Estimation of Relative Humidity from Satellites. Jour. Appl. Meteor., 6, 1088-1096.

Fujita, Tetsuya and William Bandeen, 1965: Resolution of the Nimbus High Resolution Infrared Radiometer. Jour. Appl. Meteor., 4, 492-503.

Global Atmospheric Research Programme (GARP). Report of a Study Conference held at Stockholm, Sweden, 28 June - 11 July 1967, Jointly Organized by the ICSU/IUGG - Committee on Atmospheric Sciences and COSPAR and co-sponsored by the World Meteorological Organization; 144 pp.

Goldberg, I. L., 1968: A Very High Resolution Radiometric Experiment for ATS F and G. Doc. X-622-68-26, NASA Goddard Space Flight Center.

Goldschlak, L., 1968: Nimbus III Real Time Transmission Systems. Technical Report under Contract NAS 5-10343 with Allied Research Associates, Inc.

Hanel, Rudolf A., 1961: Low Resolution Unchopped Radiometer for Satellites. ARS Journal, February, 246-250.

Hanel, R. A. and D. Q. Wark, 1961: TIROS II Radiation Experiment and Its Physical Significance. Jour. Opt. Soc. Am., 51, 1394-1399.

Hanel, R. A., W. R. Bandeen, and B. J. Conrath, 1963: The Infrared Horizon of the Planet Earth. Jour. Atmos. Sci., 20, 73-86.

Hanel, R. A. and L. Chaney, 1966: The Merits and Shortcomings of a Michelson Type Interferometer to Obtain the Vertical Temperature and Humidity Profile. Proceedings of the XVII International Astronautical Congress, Madrid, 9-15 October 1966, Vol. II. (Also available as Doc. X-620-66-476, NASA Goddard Space Flight Center.)

Hanel, R. A., 1968: Personal communication. Goddard Space Flight Center, Greenbelt, Md.

Hawkins, R. S., 1964: Analysis and Interpretation of TIROS II Infrared Radiation Measurements. Jour. Appl. Meteor. 3, 564-572.

Hilleary, D. T., D. Q. Wark, and D. G. James, 1965: An Experimental Determination of the Atmospheric Temperature Profile by Indirect Means. Nature, 205 (4970), 489-491.

Hilleary, D. T., E. L. Heacock, W. A. Morgan, R. H. Moore, E. C. Mangold, and S. D. Soules, 1966: Indirect Measurements of Atmospheric Temperature Profiles from Satellites: III. The Spectrometers and Experiments. Mo. Weather Review, 94, 367-377.

House, Frederick B., 1965: The Radiation Balance of the Earth from a Satellite. Ph.D. Thesis, Department of Meteorology, The University of Wisconsin, Madison, 69 pp. (Report to NASA under Contract NAS w-65.)

Hovis, W. A., W. A. Kley, and M. G. Strange, 1967: Filter Wedge Spectrometer for Field Use. Applied Optics, 6, 1057-1058.

Hovis, W. A. and M. Tobin, 1967: Spectral Measurements from 1.6 to 5.4 Microns of Natural Surfaces and Clouds. Applied Optics, 6, 1399-1402.

Howard, John Nelson, Darrell L. Burch, and Dudley Williams, 1955: Near-Infrared Transmission Through Synthetic Atmospheres. AFCRC-TR-55-213, Geophysical Research Papers No. 40, Air Force Cambridge Research Center, 244 pp.

James, D. G., 1967: Indirect Measurements of Atmospheric Temperature Profiles from Satellites: IV. Experiments with the Phase 1 Satellite Infrared Spectrometer. Mo. Weather Review, 95, 457-462.

Jensen, Clayton E., Jay S. Winston, and V. Ray Taylor, 1966: 500-MB Heights as a Linear Function of Satellite Infrared Radiation Data. Mo. Weather Rev., 94, 641-649.

Kaplan, Lewis E., 1959: Inference of Atmospheric Structure from Remote Radiation Measurements. Jour. Opt. Soc. Am., 49, 1004-1007.

Kennedy, James S. and William Nordberg, 1967: Circulation Features of the Stratosphere Derived from Radiometric Temperature Measurements with the TIROS VII Satellite. Jour. Atmos. Sci., 24, 711-719.

King, Jean I. F., 1956: The Radiative Heat Transfer of Planet Earth, pp. 133-136 in Scientific Uses of Earth Satellites, ed. James A. Van Allen, University of Michigan Press, Ann Arbor, 316 pp.

King, Jean I. F., 1964: Inversion by Slabs of Varying Thickness. Jour. Atmos. Sci., 21, 324-326.

Kunde, Virgil G., 1965: Theoretical Relationship Between Equivalent Blackbody Temperatures and Surface Temperatures Measured by the Nimbus High Resolution Infrared Radiometer, pp. 23-36 in Observations from the Nimbus I Meteorological Satellite. Special Publication SP-89, NASA, Washington, D.C., 90 pp.

Lienesch, J. H. and D. Q. Wark, 1967: Infrared Limb Darkening of the Earth from Statistical Analysis of TIROS Data. Jour. Appl. Meteor., 6, 674-682.

McCulloch, A. W., 1968: Personal communication. Goddard Space Flight Center, Greenbelt, Md.

McQuain, Robert H., 1967: ATS-1 Camera Experiment Successful. Bull. Am. Meteor. Soc., 48, 74-79.

Möller, Fritz, and Ehrhard Raschke, 1964: Evaluation of TIROS III Radiation Data. Contractor Report CR-112, NASA, Washington, D.C., 114 pp.

Möller, F., 1967: Eine Karte der Strahlungsbilanz des Systems Erde - Atmosphäre für Einen 14 Tägigen Zeitraum. Meteorologische Rundschau, 20 (4), 97-98.

Nelson, David F. and Robert Parent, 1965: The Prototype Flat-Plate Radiometers for the ESSA III Satellite, Chap. 6 in Annual Report-1966 WBG-27 Amendment No. 1, Department of Meteorology, The University of Wisconsin, Madison.

Nimbus II Users' Guide, 1966: National Space Science Data Center, Goddard Space Flight Center, NASA, Greenbelt, Md., 229 pp.

Nimbus III User's Guide, 1968: National Space Science Data Center, Goddard Space Flight Center, NASA, Greenbelt, Md.

Nordberg, W., W. R. Bandeen, B. J. Conrath, V. Kunde, and I. Persano, 1962: Preliminary Results of Radiation Measurements from the TIROS III Meteorological Satellite. Jour. Atmos. Sci., 19, 20-30.

Nordberg, W. and Harry Press, 1964: The Nimbus I Meteorological Satellite. Bull. Amer. Meteor. Soc., 45, 684-687.

Nordberg, William, 1965: Geophysical Observations from Nimbus I. Science, 150, 559-572 (Oct. 29).

Nordberg, W., W. R. Bandeen, G. Warnecke, and V. Kunde, 1965: Stratospheric Temperature Patterns Based on Radiometric Measurements from the TIROS 7 Satellite, pp. 782-809 in Space Research V, ed. D. G. King-Hele, P. Muller, and G. Righini. North-Holland Publishing Co., Amsterdam, 1248 pp.

Nordberg, W., A. W. McCulloch, L. L. Foshee, and W. R. Bandeen, 1966: Preliminary Results from Nimbus II. Bull. Amer. Meteor. Soc., 47, 857-872.

Operational Satellites Office, 1968: Goddard Space Flight Center, Greenbelt, Md. Personal communication.

Oxford-Reading Group, 1966: Selective Chopper Radiometer for Atmospheric Temperature Sounding for the Nimbus "D" Satellite. Joint Proposal by Oxford and Reading Universities to NASA for a Flight Experiment on Nimbus D, dated 15 April 1966.

Peckham, G., C. D. Rodgers, J. T. Houghton, and S. D. Smith, 1966: Remote Temperature Sensing of the Earth's Atmosphere Using a Selective Chopper Radiometer, in Proceedings of the Symposium on Electromagnetic Sensing of the Earth from Satellites, Miami Beach, Florida, 22-24 November 1965.

Popham, R. W. and R. E. Samuelson, 1965: Polar Exploration With Nimbus Meteorological Satellite. Arctic (Journal of the Arctic Institute of North America), 18, 246-255.

Rao, P. Krishna and Jay S. Winston, 1963: An Investigation of Some Synoptic Capabilities of Atmospheric "Window" Measurements from Satellite TIROS II. Jour. Appl. Meteor., 2, 12-23.

Raschke, Ehrhard, 1967: A Quasi-Global Analysis of the Mean Relative Humidity of the Upper Troposphere. Tellus, XIX, 214-218.

Raschke, E. and W. R. Bandeen, 1967a: A Quasi-Global Analysis of Tropospheric Water Vapor Content and Its Temporal Variations from Radiation Data of the Meteorological Satellite TIROS IV, pp. 920-931 in Space Research VII, Vol. 2, ed. R. L. Smith-Rose, North-Holland Publishing Co., Amsterdam, 1479 pp.

Raschke, Ehrhard and William R. Bandeen, 1967b: A quasi-Global Analysis of Tropospheric Water Vapor Content from TIROS IV Radiation Data. Jour. Appl. Meteor., 6, 468-481.

Raschke, Ehrhard, Fritz Möller, and William R. Bandeen, 1968: The Radiation Balance of Earth-Atmosphere System Over Both Polar Regions Obtained from Radiation Measurements of the Nimbus II Meteorological Satellite, pp. 42-57 in Scientific Papers Dedicated to Dr. Anders Ångström, Meddelanden, Serie B, Nr. 28, Sveriges Meteorologiska och Hydrologiska Institut, Stockholm. (Also available as Doc. X-622-67-460, NASA Goddard Space Flight Center.)

Raschke, Ehrhard and Musa Pasternak, 1968: The Global Radiation Balance of the Earth-Atmosphere System Obtained from Radiation Data of the Meteorological Satellite Nimbus II, in Space Research VIII, ed. A. Dollfus, North-Holland Publishing Co., Amsterdam.

Raschke, Ehrhard, 1968: The Radiation Balance of the Earth-Atmosphere System from Radiation Measurements of the Nimbus II Meteorological Satellite. Technical Note TN D-4589, NASA, Washington, D.C., 81 pp.

Rasool, S. I., 1964: Cloud Heights and Nighttime Cloud Cover from TIROS Radiation Data. Jour. Atmos. Sci., 21, 152-156.

Rasool, S. I. and C. Prabhakara, 1966: Heat Budget of the Southern Hemisphere, pp. 76-92 in Problems of Atmospheric Circulation, ed. R. V. Garcia and T. F. Malone. Spartan Books, Washington, D.C., 186 pp.

Shaw, J. H., R. A. McClatchey, and P. W. Schaper, 1967: Balloon Observations of the Radiance of the Earth Between 2100 cm^{-1} and 2700 cm^{-1}. Applied Optics, 6, 227-230.

Shen, W. C., G. W. Nicholas, and A. D. Belmont, 1968: Antarctic Stratospheric Warmings During 1963 Revealed by 15-μ TIROS VII Data. Jour. Appl. Meteor., 7, 268-283.

Staff Members, Aeronomy and Meteorology Division, Goddard Space Flight Center, 1964: TIROS VII, Radiation Data Catalog and Users' Manual: Vol. 1. National Space Science Data Center, Goddard Space Flight Center, NASA, Greenbelt, Md., 255 pp.

Suomi, V. E., 1958: The Radiation Balance of the Earth from a Satellite. pp. 331-340 in Annals of the IGY, VI, ed. L. V. Berkner. Pergamon Press, New York, 508 pp.

Suomi, V. E., 1961: The Thermal Radiation Balance Experiment on Board Explorer VII, pp. 273-305 in JUNO II Summary Project Report. Volume I, Explorer VII Satellite. Technical Note TN D-608. NASA, Washington, D.C.

Suomi, V., K. Hanson, and T. Vonder Haar, 1966: The Theoretical Basis for Low-resolution Radiometer Measurements from a Satellite, Chap. 4 in Annual Report-1966, WBG-27, Amendment No. 1, Department of Meteorology, The University of Wisconsin, Madison.

Twomey, S., 1966: Indirect Measurements of Atmospheric Temperature Profiles from Satellites: II. Mathematical Aspects of the Inversion Problem Mo. Weather Review, 94, 363-366.

Vonder Haar, Thomas H., 1968: Variations of the Earth's Radiation Budget, Ph.D. Thesis, Department of Meteorology, The University of Wisconsin, Madison, 118 pp. (Report to NASA under Contract NAS w-65.)

Wark, D. Q., 1961: On Indirect Temperature Soundings of the Stratosphere from Satellites. Jour. Geophys. Res., 66, 77-82.

Wark, D. Q., G. Yamamoto, and J. H. Lienesch, 1962: Methods of Estimating Infrared Flux and Surface Temperature from Meteorological Satellites. Jour. Atmos. Sci., 19, 369-384.

Wark, D. Q. and H. E. Fleming, 1966: Indirect Measurements of Atmospheric Temperature Profiles from Satellites: I. Introduction. Mo. Weather Review, 94, 351-362.

Wark, D. Q., F. Saiedy, and D. G. James, 1967: Indirect Measurements of Atmospheric Temperature Profiles from Satellites: VI. High-Altitude Balloon Testing, Mo. Weather Review, 95, 468-479.

Wark, D. Q., 1968: Personal communication. National Environmental Satellite Center, ESSA, Suitland, Md.

Warnecke, G., 1966a: TIROS VII 15μ Radiometric Measurements and Mid-Stratospheric Temperatures, pp. 215-227 in Satellite Data in Meteorological Research, NCAR-TN-11, ed. H. M. E. Van de Boogaard. National Center for Atmospheric Research, Boulder, Colorado, 349 pp.

Warnecke, Guenter, 1966b: Synoptic Applications of Satellite-Borne Infrared Window Measurements, pp. 121-130 in Satellite Data in Meteorological Research, NCAR-TN-11, ed. H. M. E. Van de Boogaard. National Center for Atmospheric Research, Boulder, Colorado, 349 pp.

Warnecke, Guenter, Lewis Allison, and Lonnie L. Foshee, 1968a: Observations of Sea Surface Temperatures and Ocean Currents from Nimbus II, in Space Research VIII, ed. A. Dollfus, North-Holland Publishing Co., Amsterdam.

Warnecke, Guenter, 1968b: Personal communication. Goddard Space Flight Center, Greenbelt, Md.

Warnecke, Guenter and Andrew W. McCulloch, 1968c: Stratospheric Temperature Patterns Derived from Nimbus II Measurements, in Space Research VIII, ed. A. Dollfus, North-Holland Publishing Co., Amsterdam.

Warnecke, Guenter and Wendell S. Sunderlin, 1968d: The First Color Picture of the Earth Taken from the ATS-3 Satellite. Bull. Am. Meteor. Soc., 49, 75-83.

Weinstein, Melvin and Verner E. Suomi, 1961: Analysis of Satellite Infrared Radiation Measurements on a Synoptic Scale. Mo. Weather Rev., 89, 419-428.

Widger, W. K., Jr., J. C. Barnes, E. S. Merritt, and R. B. Smith, 1965: Meteorological Interpretation of Nimbus High Resolution Infrared (HRIR) Data. Contractor Report CR-352, NASA, Washington, D.C. 150 pp.

Widger, William K., Jr., 1966: Weather from Way-Out. Weatherwise, 19, 100-111

Widger, W. K., Jr., C. W. C. Rogers, and P. E. Sherr, 1966: Looking Down on Spirals in the Sky. American Scientist, 54, 288-314.

Williamson, E. J., 1968: Personal communication. Goddard Space Flight Center, Greenbelt, Md.

Winston, Jay S. and P. Krishna Rao, 1962: Preliminary Study of Planetary-Scale Outgoing Long-Wave Radiation as Derived from TIROS II Measurements. Mo. Weather Rev., 90, 307-310.

Winston, J. S. and P. K. Rao, 1963: Temporal and Spatial Variations in the Planetary Scale Outgoing Long-Wave Radiation as Derived from TIROS II Measurements. Mo. Weather Rev., 91, 641-657.

Winston, Jay S., 1965: Comments on "Cloud Heights and Nighttime Cloud Cover from TIROS Radiation Data." Jour. Atmos. Sci., 22, 333-338.

Winston, Jay S., 1967a: Planetary-Scale Characteristics of Monthly Mean Long-Wave Radiation and Albedo and Some Year-to-Year Variations. Mo. Weather Rev., 95, 235-256.

Winston, Jay S., 1967b: Zonal and Meridional Analysis of 5-Day Averaged Outgoing Long-Wave Radiation Data from TIROS IV Over the Pacific Sector in Relation to the Northern Hemisphere Circulation. Jour. Appl. Meteor., 6, 453-463.

Wolk, M. and F. Van Cleef, 1967: Indirect Measurements of Atmospheric Temperature Profiles from Satellites: V. Atmospheric Soundings from Infrared Spectrometer Measurements at the Ground. Mo. Weather Review, 95, 463-467.

COMMENTS ON A PAPER BY W. R. BANDEEN

Comments by S. Fritz
Environmental Science Services Administration
National Environmental Satellite Center
Suitland, Maryland

The paper presented and distributed by W. R. Bandeen was entitled "Experimental Approaches to Remote Atmospheric Probing in the Infrared from Satellites." The following comments will sometimes refer to specific sections in that document.

In the absence of calibration on-board a satellite, quantitative results are often questionable. In the case of the heat budget of the earth, quantitative results depend on the difference between the large amount of outgoing energy and the almost equally large amount of solar energy absorbed by the Earth. This lack of on-board calibration applies to the hemispherical and flat plate radiometers used on Explorer VII, TIROS, and ESSA satellites, (referred to as wide-field sensors in Section 3.1 of Bandeen's paper), as well as to the medium resolution infrared radiometers on the TIROS and Nimbus series mentioned in the same section and in Table 1. In the case of Nimbus, the on-board calibration was apparently adequate in some of the long-wave channels required to investigate the radiative budget of the earth; but calibration for the solar channels was lacking, so that the energy reflected from the earth is in more question.

It is well known that the wide-angle radiometers and the TIROS medium resolution radiometers did degrade with time; and in the absence of on-board calibration required accuracy in radiation values is lacking. This does not mean that a great deal of useful information was not obtained. For the relative distribution of the field of radiation from one place to another on any one day, and even from one day to another on adjacent days during which the calibration changed little, did indeed lend itself to a much useful research involving cloud forms, cloud patterns, the earth surface temperature, stratospheric temperature, etc.

More needs to be said about the water vapor determination using the 6 micron and 10 micron channels, the results of which are displayed in Figure 4. In his oral presentation Mr. Bandeen did discuss the limitations and agreed that the determination of water vapor in the presence of high, cold clouds by this method fails. Nevertheless, the so-called results of the water vapor distribution obtained by this method are shown in Figure 4. It is fairly obvious that Figure 4 is mainly a representation of the major cloud systems; the figure merely shows that where extensive clouds with large vertical development exist, as over the major tropical continents, then the amount of water vapor in mid-troposphere is high. This result could be obtained by the use of the 10 micron channel alone, or with one of a number of other channels. A more sophisticated method is not necessary for the correlation of pattern of radiation with the pattern of relative humidity or perhaps of other water vapor parameters.

In Section 3.4, Bandeen questions the use of the 3.5 to 4.1 micron radiation for determining the surface temperatures. It is quite possible that the ocean surface temperature could be determined even in daytime in the absence of clouds. This might be true because the reflectivity of solar radiation from the ocean surface at those wavelengths might be quite small so that the emitted radiation would dominate and might yield an accurate enough surface temperature. This has apparently not yet been tried, but should be.

REMOTE ATMOSPHERIC TEMPERATURE MEASUREMENT

There was a great deal of discussion, not only in Mr. Bandeen's paper but in several other papers at the meeting in Chicago, about the determination of the vertical temperature structure from a series of radiation measurements. In principle it is not possible to derive a unique set of temperatures from a set of radiation measurements alone. A unique solution is possible only after some assumption is made about the nature of the solution. The basic difficulty can be illustrated in the following way.

The radiance, I_i, measured by a satellite, at frequency, (ν_i), is given by

$$I_i = \int_0^1 B(\nu_i, T)\, d\tau(\nu_i) = \int_{\log p_o}^{\log 0.1} B \frac{\delta \tau}{\delta \log p}\, d \log p \qquad (1)$$

where the symbols have standard meanings, and the "top of the atmosphere" is assumed to be at p = 0.1 mb; this is an adequate "top" for the 15μ CO_2 band with resolution of about 5 cm^{-1}.

Now, for purposes of illustration, suppose we make measurements at two frequencies, "a" and "b". Assume that the Planck functions, B, have been normalized to a given reference frequency, and that we require the average temperature for two layers of the atmosphere. The average Planck function, $\overline{B}$, will be closely related to the average temperatures in the layers. Therefore, from equation (1),

$$I_a = \left[\overline{B \frac{\delta \tau_a}{\delta \log p}}\, \Delta \log p\right]_H + \left[\overline{B \frac{\delta \tau_a}{\delta \log p}}\, \Delta \log p\right]_L \qquad (2)$$

$$I_b = \left[\overline{B \frac{\delta \tau_b}{\delta \log p}}\, \Delta \log p\right]_H + \left[\overline{B \frac{\delta \tau_b}{\delta \log p}}\, \Delta \log p\right]_L \qquad (3)$$

where "H" refers to the higher layer and "L" refers to the lower layer. The normalization factors for frequency have been incorporated into I_a and I_b. The averages have been performed with respect to log p.

Now

$$\overline{B\left(\frac{\delta \tau_a}{\delta \log p}\right)} = \bar{B}\overline{\left(\frac{\delta \tau_a}{\delta \log p}\right)} + \overline{B'\left(\frac{\delta \tau_a}{\delta \log p}\right)'}$$

where the primes refer to deviations from the average. Since

$$\overline{\left(\frac{\delta \tau_a}{\delta \log p}\right)} \Delta \log p = \Delta \tau_a$$

equation (2) becomes

$$I_a = \left[\bar{B}\ \Delta\tau a\right]_H + \left[\bar{B}\ \Delta\tau a\right]_L + \left[\overline{B'\left(\frac{\delta\tau_a}{\delta \log p}\right)'}\ \Delta \log p\right]_H + \left[\overline{B'\left(\frac{\delta \tau_a}{\delta \log p}\right)'}\ \Delta \log p\right]_L \quad (4)$$

with a corresponding equation for equation (3).

The solutions for $\bar{B}_H$ and $\bar{B}_L$ are, in matrix notation,

$$\begin{pmatrix}\bar{B}_H \\ \bar{B}_L\end{pmatrix} = A^{-1} \begin{pmatrix}I_a \\ I_b\end{pmatrix} - A^{-1}\begin{pmatrix}V_a \\ V_b\end{pmatrix} \quad (5)$$

Here, A^{-1} is the inverse of matrix A;

$$A = \begin{pmatrix}\Delta\tau_{aH} & \Delta\tau_{aL} \\ \Delta\tau_{bH} & \Delta\tau_{bL}\end{pmatrix}$$

and V_a is the sum of the last two terms in equation (4); V_b is the corresponding term in the equation involving frequency b.

From equation (5), it is thus evident that even without errors in the measured radiances, and even if only two average temperatures are sought from two spectral measurements, additional information is required in order to evaluate $\overline{B}_H$ or $\overline{B}_L$. The additional information required is a knowledge of the magnitude of the terms V_a and V_b. These involve the co-variance between B' and $(\delta T/\delta \log p)'$, at the two frequencies. This co-variance term may perhaps be estimated from climatological data, or from synoptic data where radiosonde measurements exist. Perhaps it is sufficiently well correlated with $\overline{B}$ itself or with the radiances. At any rate some estimate of it would be required.

From measurements at a few additional frequencies, additional average temperatures at a correspondingly larger number of layers can be evaluated. But always terms such as V_a will appear.

Where the number of levels, at which temperature is estimated, exceeds the number of radiances measured, it is even more obvious that some additional assumption is required. In practice, climatological data obtained from a long record of radiosonde data, or from a few days of actual radiance measurements over radiosonde stations, can serve to aid in acquiring the desired temperatures, if the radiances are sufficiently accurate. This was mentioned by several people at the Panel Discussions in Chicago.